AD-A072 942 ORINCON CORP LA JOLLA CALIF F/G 17/1
FURTHER DEVELOPMENT AND NEW CONCEPTS FOR BIONIC SONAR. VOLUME 3--ETC(U)
OCT 78 R A ALTES, R W FLOYD N66001-78-C-0080
UNCLASSIFIED OC-R-78-A004-1-VOL-3 NOSC-TR-404-VOL-3 NL

1 OF 1
AD A072 942

END
DATE FILMED
9-79
DDC

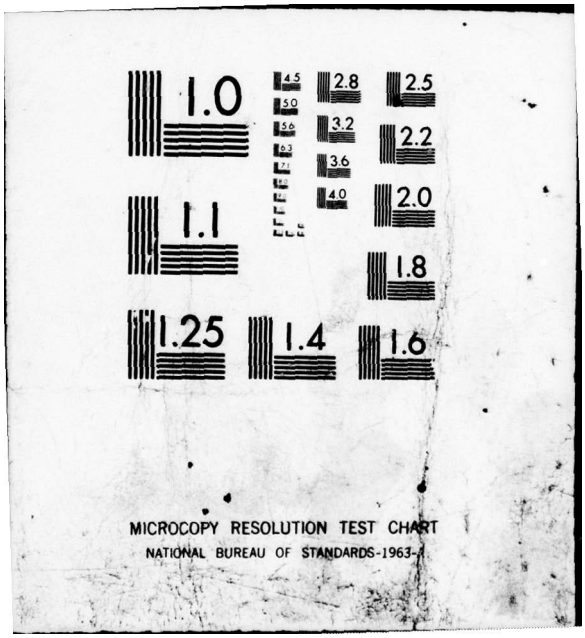
1.0
1.1
1.25
1.4
1.6
1.8
2.0
2.2
2.5
2.8
3.2
3.6
4.0
4.5
5.0
5.6
6.3
MICROCOPY RESOLUTION TEST CHART
NATIONAL BUREAU OF STANDARDS-1963-A

NOSC

NOSC TR 404
VOLUME 3

NOSC TR 404
VOLUME 3

Technical Report 404

FURTHER DEVELOPMENT AND NEW CONCEPTS FOR BIONIC SONAR

Volume 3 - New Concepts and Experiments

RA Altes
ORINCON Corporation
RW Floyd, NOSC
(Contract Monitor)

October 1978

Approved for public release; distribution unlimited

NAVAL OCEAN SYSTEMS CENTER
SAN DIEGO, CALIFORNIA 92152

NAVAL OCEAN SYSTEMS CENTER, SAN DIEGO, CA 92152

AN ACTIVITY OF THE NAVAL MATERIAL COMMAND

RR GAVAZZI, CAPT, USN
Commander

HL BLOOD
Technical Director

ADMINISTRATIVE INFORMATION

The work reported here was performed by Richard A. Altes, ORINCON Corporation, 3366 No. Torrey Pines Ct., Suite 320, La Jolla, CA 92037 under Contract Number N66001-78-C-0080. R. W. Floyd, Code 512, was the contract monitor.

The work was reported in three volumes. This document contains volume 3 of the report, reproduced in its entirety.

Released by

Dr. JF FISH, Head
Bioacoustics and Bionics Division

Under authority of

HO PORTER, Head
Biosciences Department

UNCLASSIFIED

SECURITY CLASSIFICATION OF THIS PAGE (When Data Entered)

(19) REPORT DOCUMENTATION PAGE

READ INSTRUCTIONS BEFORE COMPLETING FORM

(18) 1. REPORT NUMBER: NOSC TR-404 Volume-3 (9) Final rept.

2. GOVT ACCESSION NO.

3. RECIPIENT'S CATALOG NUMBER

(6) 4. TITLE (and Subtitle)

FURTHER DEVELOPMENT AND NEW CONCEPTS FOR BIONIC SONAR.
VOLUME 3 - NEW CONCEPTS AND EXPERIMENTS.

5. TYPE OF REPORT & PERIOD COVERED

FINAL FY 78

(14) 6. PERFORMING ORG. REPORT NUMBER

OC-R-78-A004-1 Vol-3

7. AUTHOR(s)

RA Altes, ORINCON Corporation
RW Floyd, NOSC (Contract Monitor)

8. CONTRACT OR GRANT NUMBER(s)

(15) N66001-78-C-0080

9. PERFORMING ORGANIZATION NAME AND ADDRESS

ORINCON CORPORATION
3366 No. Torrey Pines Ct., Suite 320
La Jolla, CA 92037

10. PROGRAM ELEMENT, PROJECT, TASK AREA & WORK UNIT NUMBERS

PE6271; SF11-121-491

11. CONTROLLING OFFICE NAME AND ADDRESS

Naval Ocean Systems Center, Hawaii Laboratory
PO Box 997
Kailua, Hawaii 96734

(11) 12. REPORT DATE

October 1978

13. NUMBER OF PAGES

66

14. MONITORING AGENCY NAME & ADDRESS (if different from Controlling Office)

NAVSEA 0342 (F. Romano)
2221 Jefferson Davis Highway
Arlington, VA 22314

15. SECURITY CLASS. (of this report)

Unclassified

15a. DECLASSIFICATION/DOWNGRADING SCHEDULE

(10) Richard A. Altes
R. W. Floyd

16. DISTRIBUTION STATEMENT (of this Report)

Approved for public release; distribution unlimited.

(12) 41 p.

17. DISTRIBUTION STATEMENT (of the abstract entered in Block 20, if different from Report)

(16) F11121

18. SUPPLEMENTARY NOTES

(17) SF1112L491

19. KEY WORDS (Continue on reverse side if necessary and identify by block number)

Bionics
Optimum detectors
Signal processing
Sonar
Spectrogram correlation
Target transfer function

20. ABSTRACT (Continue on reverse side if necessary and identify by block number)

This report documents theoretical studies of models for echolocation signal processing of dolphins and the testing of the effectiveness of these models for detecting and classifying small objects in introduced noise and reverberation. This volume investigates potential uses of binaural (two-receiver) sonar systems. The effective beamwidth for a two-receiver array is computed by using a range ambiguity function. Effective beamwidth decreases as array size and bandwidth increase, so a trade-off can be made between

→ next page

(Continued)

DD FORM 1 JAN 73 1473 EDITION OF 1 NOV 65 IS OBSOLETE
S/N 0102-LF-014-6601

UNCLASSIFIED

SECURITY CLASSIFICATION OF THIS PAGE (When Data Entered)

392776

20. (Continued)

array size and bandwidth. Binaural systems may also be used to estimate cross-range velocity. Expected error for velocity estimation is computed for surveying certain range, bandwidth, receiver separation and SNR parameters.

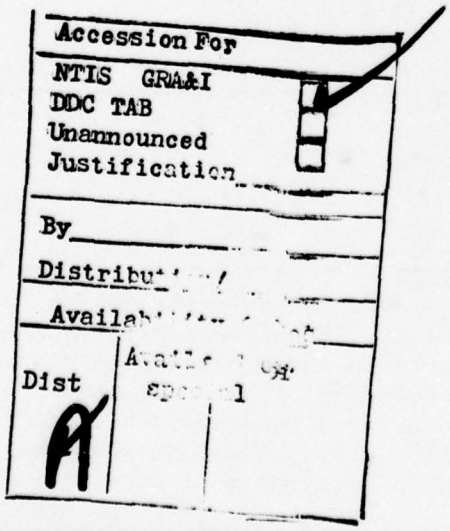

TABLE OF CONTENTS

Volume 3. NEW CONCEPTS AND EXPERIMENTS

TABLE OF CONTENTS (Continued)

III. NEW CONCEPTS AND EXPERIMENTS

3.1 Introduction

This volume describes some new hypotheses and experiments that are relevant to animal echolocation and to man made sonar systems.

The first hypothesis is that some echolocating animals may use very wide signal bandwidths in order to compensate for a relatively small array that has only two transducers. This hypothesis depends upon the assumption that a trade-off exists between array size and signal bandwidth. The existence of such a trade-off is investigated by devising a new ambiguity function that applies to range and angle measurements, i.e., to estimates of a target's position in space. An effective beam width can be defined in terms of the new ambiguity function, and it is found that this beam width decreases as the array is made larger (the classical result) and also as signal bandwidth is increased (a new result). A trade-off between array size and signal bandwidth therefore does exist for a given required effective beam width. This result supports the hypothesis that the use of large signal bandwidths by dolphins and some bats may serve to compensate for a limited array size. The result may also have considerable impact upon the design of future man made sonar systems.

The second hypothesis is that bats (and dolphins) may be able to estimate cross-range velocity with sufficient accuracy to compensate for evasive maneuvers by moths (and fish). This hypothesis can be investigated by studying the dependence of expected error in a cross-range velocity estimate upon parameters such as

range, interaural distance, and signal-to-noise ratio. It is shown that cross-range velocity estimation is indeed a feasible process for targets that are less than one meter from the animal, where estimation of evasive maneuvers becomes critical.

The third hypothesis involves the Johnson-Titlebaum model of echolocation by energy spectrum analysis. The hypothesis is that locally optimum detection is used to determine the presence or absence of a target by investigation of the energy spectrum. The energy spectrum is obtained by Fourier analysis of data over a long integration time that includes both the transmitted signal and the target echo. The locally optimum detector correlates samples of the energy spectrum with corresponding samples that would be measured in the absence of noise. The noise-free samples correspond to a ripple or sinusoidal amplitude modulation of the energy spectrum, where the period of the ripple is determined by target range. The locally optimum test for a target at a sequence of hypothesized ranges therefore involves correlation of the energy spectrum with a sequence of sinusoids, i.e., Fourier analysis of the energy spectrum. This hypothesis suggests that the Johnson-Titlebaum processor is particularly sensitive to background noise with rippled power spectrum, where the period of the ripple corresponds to the range of a target. Since a matched filter is comparatively impervious to spectral ripple, we have the basis for a behavioral experiment that can distinguish between the Johnson-Titlebaum and matched filter models of animal echolocation.

Section 3.2 describes the new range-angle ambiguity function and the bandwidth-array size trade-off. Section 3.3 presents

a feasibility argument in support of the hypothesis that echolocating animals can measure cross-range velocity. Section 3.4 discusses the locally optimum detector for energy spectrum analysis and an experiment to test the Johnson-Titlebaum echolocation model.

3.2 The Trade-Off Between Array Size and Signal Bandwidth, and Its Possible Utilization in Animal Echolocation

3.2.1 Brief Summary of Section 3.2

Target position estimation in radar and sonar means joint estimation of range and angle in the presence of noise and clutter. The global behavior of a maximum likelihood position estimator, and the clutter suppression capability of the system, can be written in terms of a range-angle ambiguity function. This function depends upon signal waveform and array configuration, i.e., upon both temporal and spatial characteristics of the system.

Ambiguity and variance bound analysis indicates that system bandwidth can often be traded for array size, and direction-dependent signals can be used to obtain better angle resolution without increasing the size of the array. Wideband, direction-dependent signals (temporal diversity) can be traded for large real or synthetic arrays (spatial diversity). This trade-off is apparently exploited by some animal echolocation systems.

The above insights are obtained mostly from the properties of the range-angle ambiguity function. In general, an appropriate ambiguity function should be very useful for the design and evaluation of any maximum likelihood parameter estimator. System identification methods and radio navigation systems, for example, can be optimized by minimizing the volume of a multiparameter ambiguity function.

3.2.2 Introduction

System requirements for radar, sonar, or diagnostic ultrasound include parameters such as array size, signal bandwidth, and processor complexity (measured by the time-bandwidth product of the signal, data storage capacity, and processing time). System performance involves quantities such as estimator variance, resolution, and clutter rejection capability. Performance can be measured in terms of Cramér-Rao (CR) bounds, ambiguity function properties, and signal-to-clutter ratio. If these performance measures can be written in terms of array size, signal bandwidth, and processor complexity (system requirements), then trade-offs between requirements such as array size and bandwidth can be assessed.

CR bounds[1,2] provide a local measure of estimator accuracy for particular values of the estimated parameters. In terms of a hypothesis test, CR bounds are useful when the hypothesized parameters are nearly equal to their true values, i.e., when there is good prior information about the parameters that are to be estimated. CR bounds are often obtained by assuming that the data consists of a signal that depends upon the unknown parameters, added to white, Gaussian noise (WGN). If the data actually consists of additional, spurious signals (clutter), then the WGN assumption is invalid, and meaningful CR bounds can be obtained only after a more general probability distribution has been worked out.

The ambiguity function[3,4] illustrates the global properties of a maximum likelihood (ML) estimator. In terms of a hypothesis test, the ambiguity function shows the response of the estimator to all possible values of the hypothesized parameters, when the true parameters are specified. Possible confusion between different

parameter values can thus be illustrated. Like CR bounds, the ambiguity function is often derived under a WGN assumption, but the effect of spurious echoes can be analyzed in terms of this idealized ambiguity function, and its utility is not restricted to the WGN case.[5-10] In view of these properties, it is not surprising that ambiguity analysis often results in the imposition of constraints upon a system design that minimizes a CR bound. For example, the ambiguity function gives the accuracy of prior knowledge that is required for such a system.

We shall consider properties of both CR bounds and the ambiguity function for joint range-angle estimation. Targets that are in the near field of an array, as well as the far field, will be considered, since the effective size of synthetic aperture arrays is so large that the far field assumption is often violated. Diagnostic ultrasound arrays for examination of near-surface effects (breast and parotid tumors, carotid artery wall thickness) will also sometimes operate in a near-field configuration.

The ambiguity function approach to radar/sonar signal design is well established,[46] and this paper uses a similar method for combined signal and array (temporal and spatial) design. Ambiguity analysis, however, has apparently been neglected for other parameter estimation problems, and it has been confined to the radar/sonar literature. One purpose of this paper is to illustrate the advantages of multiparameter ambiguity analysis[45] in a more general context.

It will be shown that the volume of the ambiguity function provides a measure of the extent to which different parameter estimates can be separated from each other and from a background that may include spurious signals as well as noise. By far the best known ambiguity function is associated with delay and frequency shift measurements, using narrowband signals.[3] The volume of this ambiguity function depends only upon signal energy, and the resulting volume

invariance for energy-normalized signals can be interpreted as a radar uncertainty principle.[27] The volume invariance of the narrow-band range-Doppler ambiguity function is more the exception than the rule, however,[14,15] and the analysis in this paper demonstrates that minimization of ambiguity volume can be an important technique for the optimization of a parameter estimator. Minimization of ambiguity volume should be especially applicable to signal design for system identification, a branch of control theory that has much in common with radar/sonar design.

Animal sonar or echolocation is a biological phenomenon that is especially fascinating to radar/sonar engineers. One of the first proposals for a man-made sonar system was suggested in 1912, after the Titanic disaster, as a simulation of "the sixth sense of the bat."[26,28] Photographs of bats in pursuit of insects among foliage[29] seem to indicate a high degree of clutter suppression capability, and the echolocation performance of cetaceans in shallow, reverberation-limited environments is also impressive. Animal sonars operate under a significant constraint; their receiving "arrays" consist of only two closely spaced elements. Many echolocating animals, however, have evolved extremely wideband systems, and the highest frequency can be as much as a factor of ten larger than the lowest frequency.[20] We know that increasing a signal's bandwidth results in better range resolution[3,4] and better target discrimination capability,[30-35] and that large time-bandwidth products can be advantageous for wideband velocity resolution[36,37] or for Doppler tolerance.[38-40] We also suspect that the use of wideband signals may be associated with better angle measurements,[11,21] and that echo-locating animals may be able to compensate for limited array size by using larger bandwidths. The following analysis indicates that this suspicion is well-founded.

For the reader who is interested in radar, sonar, diagnostic ultrasound, and animal echolocation, the paper should provide some useful results and insights. For the reader who is interested in other parameter estimation problems, the specific results are not so important, but the general approach illustrates a useful system design philosophy.

3.2.3 Problem Formulation and General Results

In this section, expressions for CR bounds and the ambiguity function are derived for the position estimation problem. The results will apply to all planar array configurations. No assumptions about array shape or target position will be introduced, except for the simplifying assumption that the target lies in the plane of the receiving array.

Let $E(\omega)$ be the Fourier transform of an echo, measured at the target. The frequency domain response of the k^{th} array element to the echo is:

$$F_k(\omega) = A_k E(\omega) \exp(-j\omega\tau_k) \tag{1}$$

where

$$A_k \equiv \text{complex gain of the } k^{th} \text{ element} \tag{2}$$

$$\tau_k \equiv \text{delay from target to } k^{th} \text{ element .} \tag{3}$$

Let L be a straight line segment between the elements of the array that are furthest apart. The range parameter τ is defined as the delay between the target and the center point P of L, i.e., the point that lies midway between the extremities of the array (see Figure 1). The direction parameter θ is defined to be the angle between the normal to L at P and the line segment between P and the target. Movement of the target counterclockwise around P causes θ to increase, i.e., θ is positive in the counterclockwise direction.

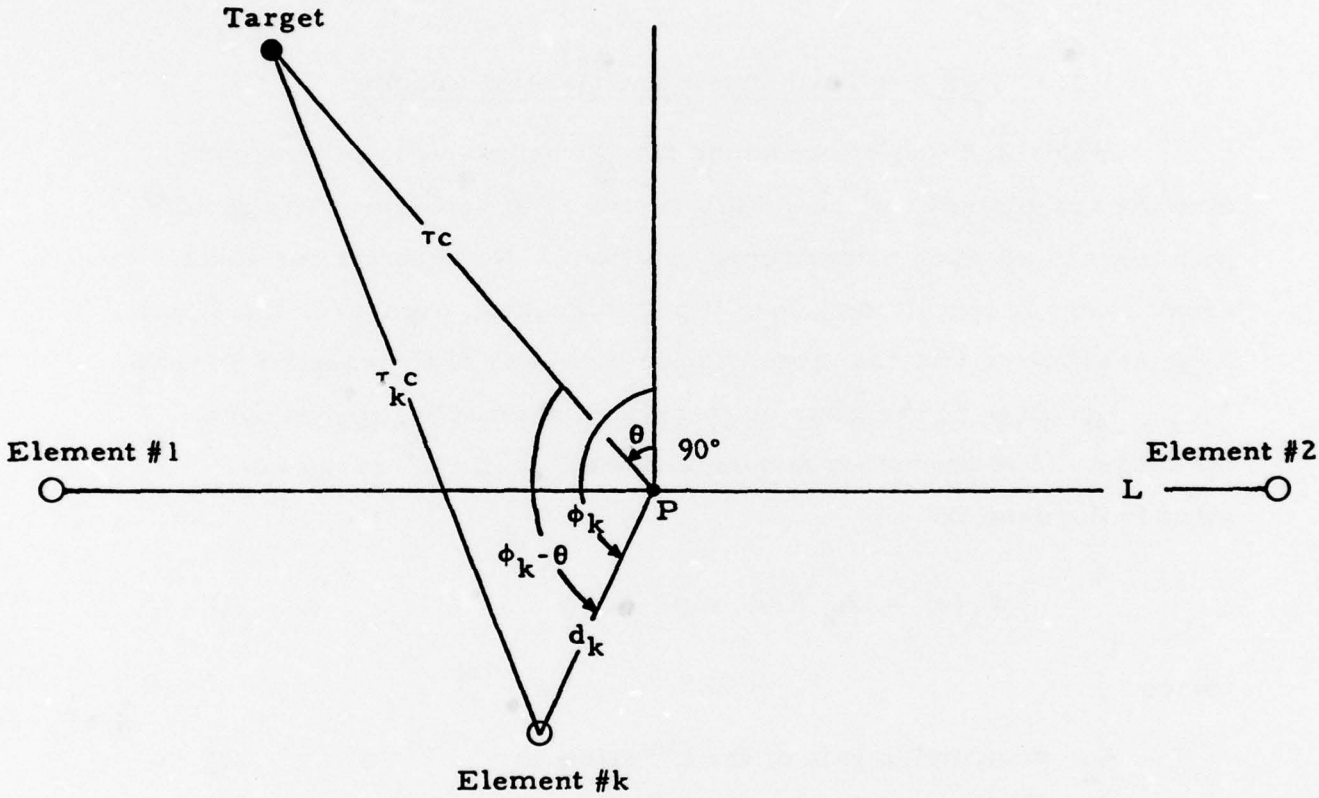

Figure 1. Definitions of angles and distances for a planar array of receiving elements.

The position of each array element can be defined in the same way as the target position. In Figure 1, the k^{th} element position is described in terms of the direction parameter ϕ_k and the distance d_k from P, where ϕ_k is the angle between the normal to L at P and the line segment between P and the array element. From Figure 1, a general expression for τ_k is

$$\tau_k = [\tau^2 + (d_k/c)^2 - 2\tau (d_k/c) \cos(\phi_k - \theta)]^{1/2} \qquad (4)$$

and τ_k depends upon the unknown parameters τ and θ, as well as upon the known parameters d_k and ϕ_k.

The array element responses in the absence of noise can be represented by a column vector $\underline{m}(\tau, \theta)$ of complex numbers. The first N elements of $\underline{m}(\tau, \theta)$ are frequency samples of $F_1(\omega)$ in (1). The next N elements are samples of $F_2(\omega)$, etc. In representing $F_k(\omega)$ by N frequency samples, it is implicitly assumed that the response of the k^{th} element is time limited. Although a time limited signal cannot be band limited, it is assumed that, for any acceptable mean square error $\epsilon > 0$ between the original time signal and the time signal that is reconstructed from N frequency components, there exists a bounded number N such that the mean square reconstruction error is less than ϵ. For an integration interval T, the N discrete frequency samples are separated by π/T rad/sec. For K array elements, $\underline{m}$ has KN elements.

In Gaussian noise, a data vector $\underline{r}$ is observed, where the elements of $\underline{r}$ are the frequency samples of $F_1(\omega), F_2(\omega), \ldots, F_K(\omega)$ when noise has been added to the echo. The conditional probability density function of the noisy data is[11]

$$p(\underline{r}|\tau,\theta) = (\pi^{KN/2}|\underline{\underline{C}}|)^{-1} \exp\{-[\underline{r} - \underline{m}(\tau,\theta)]^* \underline{\underline{Q}}[\underline{r} - \underline{m}(\tau,\theta)]\} \quad (5)$$

where $\underline{\underline{C}} = \underline{\underline{Q}}^{-1}$ is the noise covariance matrix and the asterisk denotes a conjugate-transpose operation.

In the presence of multiple targets and clutter or reverberation, as well as noise, it is still possible to use a Gaussian pdf as in (5), provided that an appropriate covariance matrix is determined.[12] The pdf in (5) may appear to be unrealistic for sea clutter, since the envelope of a Gaussian clutter process is Rayleigh distributed, while the measured pdf of envelope detected sea clutter echoes is often more log-normal than Rayleigh.[41,42] The empirical log-normal model for the clutter envelope indicates that the underlying pdf of the time domain clutter process decreases more slowly in the "tails" than the Gaussian distribution. The use of a frequency domain representation in (5), however, implies that time domain echoes are effectively passed through a bank of narrowband filters with impulse responses that are T seconds long. The sampled responses $\underline{r}$ of these filters tend to be much more Gaussian than the original time domain distribution.[43]

Maximum likelihood (ML) estimates of range and angle are the values of τ,θ that maximize $p(\underline{r}|\tau,\theta)$ in (5), for a given data vector $\underline{r}$. The asymptotic variance of these estimates for many observations of the data can be obtained from the matrix CR bound.[1,2] The CR bound is defined for a particular value of τ,θ, and it does not take account of the possibility that two very different parameter pairs τ_1,θ_1 and τ_2,θ_2 may yield nearly equal local maxima of $p(\underline{r}|\tau,\theta)$. The ambiguity function is a global measure of ML estimator performance that reveals the parameter pairs which are most likely to be confused with one another, i.e., which are associated with an ambiguous interpretation of the data. We shall

obtain general expressions for both the CR bound and the ambiguity function.

When range τ and angle θ are both unknown, CR bounds for their joint estimates are determined by inverting the Fisher information matrix, $\underline{\underline{J}}$. The elements of $\underline{\underline{J}}$ are

$$
\begin{aligned}
J_{11} &= J_{\tau\tau} = -E[(\partial^2/\partial\tau^2) \ln p(\underline{r} \mid \tau, \theta)] \\
J_{12} &= J_{\tau\theta} = -E[(\partial^2/\partial\tau\,\partial\theta) \ln p(\underline{r} \mid \tau, \theta)] \\
J_{21} &= J_{\theta\tau} = -E[(\partial^2/\partial\theta\,\partial\tau) \ln p(\underline{r} \mid \tau, \theta)] \\
J_{22} &= J_{\theta\theta} = -E[(\partial^2/\partial\theta^2) \ln p(\underline{r} \mid \tau, \theta)] \; .
\end{aligned}
\tag{6}
$$

Substituting (5) into (6), we obtain

$$
\begin{aligned}
J_{\tau\tau} &= 2\partial\underline{m}^*/\partial\tau \; \underline{\underline{Q}} \; \partial\underline{m}/\partial\tau \\
J_{\tau\theta} &= 2\,\mathrm{Re}\{\partial\underline{m}^*/\partial\tau \; \underline{\underline{Q}} \; \partial\underline{m}/\partial\theta\} \\
J_{\theta\tau} &= 2\,\mathrm{Re}\{\partial\underline{m}^*/\partial\theta \; \underline{\underline{Q}} \; \partial\underline{m}/\partial\tau\} \\
J_{\theta\theta} &= 2\partial\underline{m}^*/\partial\theta \; \underline{\underline{Q}} \; \partial\underline{m}/\partial\theta
\end{aligned}
$$

where $\underline{m} = \underline{m}(\tau, \theta)$ are the expected responses in (5), i.e., frequency samples of $F_k(\omega)$ in (1), for $k = 1, 2, \ldots, K$. The derivatives in (7) are evaluated at the particular τ and θ values that correspond to the target's true position. The diagonal terms of $\underline{\underline{J}}^{-1}$ are the CR bounds for the variance of the range and angle estimates $\hat{\tau}$ and $\hat{\theta}$,

$$\text{Var}\,(\hat{\tau} - \tau) \geq \left[J_{\tau\tau} - (J_{\tau\theta}\, J_{\theta\tau} / J_{\theta\theta})\right]^{-1}$$

$$\text{Var}\,(\hat{\theta} - \theta) \geq \left[J_{\theta\theta} - (J_{\tau\theta}\, J_{\theta\tau} / J_{\tau\tau})\right]^{-1} . \qquad (8)$$

In order to obtain simple mathematical expressions for the above variances, it will be assumed that

$$\underline{\underline{Q}} = N_o^{-1}\, \underline{\underline{I}} \qquad (9)$$

where N_o is the noise power spectral density and $\underline{\underline{I}}$ is the identity matrix. This assumption means that the noise is white and Gaussian, and that the noise at each of the K array elements is statistically independent of the noise at any other element. The CR bounds that are obtained by using (9) are generally not relevant for an environment that includes multiple targets and clutter or reverberation, although it may be possible to approximate a diagonal covariance matrix by using a large integration time T for the computation of the frequency domain samples $\underline{r}$.[44] The WGN assumption yields idealized bounds that convey only qualitative information about the relation between system requirements and performance. These qualitative insights, however, can be very important. For example, CR bounds for WGN show that the accuracy of angle estimates are not completely determined by the physical beamwidth of the receiver.[11]

Substituting (9) into (7), we have

$$J_{\tau\tau} = 2 N_o^{-1}\, (T/\pi) \int_{-\infty}^{\infty} \omega^2 |E(\omega)|^2\, d\omega \sum_{k=1}^{K} |A_k|^2 (\partial\tau_k / \partial\tau)^2 \qquad (10a)$$

$$J_{\tau\theta} = J_{\theta\tau} = 2N_o^{-1}(T/\pi)\int_{-\infty}^{\infty}\omega^2|E(\omega)|^2\,d\omega\sum_{k=1}^{K}|A_k|^2 \qquad (10b)$$

$$\cdot\,(\partial\tau_k/\partial\tau)\;(\partial\tau_k/\partial\theta)$$

$$J_{\theta\theta} = 2N_o^{-1}(T/\pi)\int_{-\infty}^{\infty}\omega^2|E(\omega)|^2\,d\omega\sum_{k=1}^{K}|A_k|^2\,(\partial\tau_k/\partial\theta)^2\,. \qquad (10c)$$

In (10), τ_k is given by (4) and is shown in Figure 1. Further simplifications can be obtained under appropriate assumptions about the relative magnitudes of τ, τ_k, and d_k/c. Some of these simplifications will be discussed in the sequel.

A range-angle ambiguity function is obtained by studying the behavior of the conditional probability density function when we try to determine maximum likelihood estimates by trial-and-error. This procedure has been utilized by Urkowitz, Hauer, and Koval[13] to derive an angular ambiguity function, $\chi(\theta, \theta_H)$.

The ML estimates τ, θ are the values of the hypothesized range and angle τ_H, θ_H that maximize $p[\underline{r}|\tau_H, \theta_H]$ or that minimize

$$\varepsilon = [\underline{r} - \underline{m}(\tau_H, \theta_H)]^* \underline{\underline{Q}}\,[\underline{r} - \underline{m}(\tau_H, \theta_H)] \qquad (11)$$

where

$$\underline{r} = \underline{m}(\tau, \theta) + \underline{n}$$

and where $\underline{n}$ is a vector of zero mean, complex noise samples.

Assuming that (9) is true, $E\{\varepsilon\}$ is the mean square error between $\underline{r}$ and $\underline{m}(\tau_H, \theta_H)$. Since

$$\underline{m}^*(\tau, \theta)\,\underline{m}(\tau, \theta) = \sum_{k=1}^{K}\sum_{n=1}^{N}\left|F_k(\omega_n)\right|^2 \qquad (12)$$

we see from (1) that $\left\| \underline{m}(\tau, \theta) \right\|$ does not depend upon τ_k, and it is therefore invariant in τ and θ. It follows that $E(\epsilon)$ is minimized when $\chi(\tau, \tau_H, \theta, \theta_H)$ is maximized, where

$$\chi(\tau, \tau_H, \theta, \theta_H) \propto \mathrm{Re}\left\{ \underline{m}^*(\tau, \theta) \underline{\cdot} \underline{m}(\tau_H, \theta_H) \right\}$$

$$\equiv \sum_{k=1}^{K} |A_k|^2 (1/2\pi) \int_{-\infty}^{\infty} |E(\omega)|^2$$

$$\exp\left[j\omega(\tau_k - \tau_{Hk}) \right] d\omega$$

$$= \sum_{k=1}^{K} |A_k|^2 R(\tau_k - \tau_{Hk}) \qquad (13)$$

where $R(\tau)$ is the autocorrelation function of the echo and, from (4),

$$\tau_{Hk} = \left[\tau_H^2 + (d_k/c)^2 - 2\tau_H (d_k/c) \cos(\phi_k - \theta_H) \right]^{\frac{1}{2}}. \qquad (14)$$

The trial-and-error ML estimator can be conceptualized as a large number of estimators, each matched to a different set of values of the unknown parameters. The ambiguity function $\chi(\tau, \tau_H, \theta, \theta_H)$ is the output of these estimators when a noise-free signal is present at the input to the system. If the ambiguity function is large for more than one set of hypothesized parameter values (τ_H, θ_H), then the introduction of noise can easily lead to erroneous estimates.

The range-angle ambiguity function in (13) was obtained under the WGN assumption (9). Unlike the CR bound for WGN, the ambiguity function in (13) can be applied to the analysis of system performance in the presence of clutter or reverberation and multiple targets.[5-10] If a point target is at position τ, θ and a point clutter

reflector is at position τ_c, θ_c, the output power of a correlation processor due to the clutter reflector is

$$\text{clutter response } (\tau, \theta) \propto \left| \chi(\tau, \tau_c, \theta, \theta_c) \right|^2 . \tag{15}$$

The expected output power due to a superposition of statistically independent clutter reflectors is

$$P_C = E\left\{\text{clutter response } (\tau, \theta)\right\} \propto \int_{-\pi}^{\pi} \left[\int_{-\infty}^{\infty} p(\tau_c, \theta_c) \left| \chi(\tau, \tau_c, \theta, \theta_c) \right|^2 d\tau_c \right] d\theta_c \tag{16}$$

where $p(\tau_c, \theta_c)$ is a probability density function[5] or scattering function[9] that describes the distribution of clutter in range-angle space.

The correlator response to the target is

$$P_T \propto \left| \chi(\tau, \tau, \theta, \theta) \right|^2 \tag{17}$$

and the signal to clutter ratio is

$$SCR = P_T / P_C . \tag{18}$$

For the case when $p(\tau_c, \theta_c)$ is uniform, e.g., when there is no prior knowledge of the clutter distribution, we have

$$SCR^{-1} = P_C / P_T = \text{normalized volume of } \left| \chi(\tau, \tau_H, \theta, \theta_H) \right|^2 . \tag{19}$$

One of the well-known properties of the narrowband range-velocity ambiguity function is volume invariance, i.e., the same

ambiguity volume is obtained for any energy normalized signal.[3] It would appear that this volume invariance property does not apply to other ambiguity functions, however, e.g., the wideband range-velocity ambiguity function[14,15] and the function in (13). In fact, we shall show that range-angle ambiguity volume and SCR depend upon the bandwidth of the radar/sonar system.

An effective beamwidth can also be written in terms of (16). For a target at angle θ, the expected response from clutter at angle θ_c, integrated over range, is the bracketed integral in (16). If this integral is small relative to P_T, then the effective beam pattern has small gain at θ_c when the center of the beam is aimed at the target. For uniformly distributed clutter,

$$\text{Effective angular attenuation between } \theta \text{ and } \theta_c = P_T^{-1} \int_{-\infty}^{\infty} |\chi(\tau, \tau_c, \theta, \theta_c)|^2 \, d\tau_c \, . \qquad (20)$$

We have now obtained expressions for CR bounds and the range-angle ambiguity function, under a WGN assumption. The general target and array description in Figure 1 has led to comparatively simple notation in (10) and (13), where no assumptions about specific geometries have been introduced (except for a planar array with a coplanar target). These expressions will now be applied to position measurements with a linear array.

3.2.4 Linear Array, Far Field

For a linear array, we have $\phi_k = \pm\pi/2$ for all K array elements. For simplicity of notation, we shall set $\phi_k = -\pi/2$ and we shall allow d_k to be negative as well as positive. In this case, (4) becomes

$$\tau_k = \tau\left[1 + \tau^{-2}(d_k/c)^2 + 2\tau^{-1}(d_k/c)\sin\theta\right]^{\frac{1}{2}} \tag{21}$$

If the target is in the far field, we can assume that

$$(d_k/c)^2 \ll \tau^2 \tag{22}$$

and (21) becomes

$$\tau_k \approx \tau + (d_k/c)\sin\theta\ . \tag{23}$$

Substituting (23) into (10) gives

$$J_{\tau\tau} = \text{SNR}\ D_\omega^2 \tag{24a}$$

$$J_{\theta\theta} = \text{SNR}\ D_\omega^2\ D_A^2 \cos^2\theta \tag{24b}$$

$$J_{\tau\theta}\ J_{\theta\tau} = (\text{SNR}\ D_\omega^2\ M_A \cos\theta)^2 \tag{24c}$$

where

$$\text{SNR} = (T/\pi N_o) \sum_{k=1}^{K} |A_k|^2 \int_{-\infty}^{\infty} |E(\omega)|^2\, d\omega \tag{25}$$

$$D_\omega^2 = \int_{-\infty}^{\infty} \omega^2\ |E(\omega)|^2\, d\omega \Big/ \int_{-\infty}^{\infty} |E(\omega)|^2\, d\omega \tag{26}$$

$$D_A^2 = \sum_{k=1}^{K} (d_k/c)^2\ |A_k|^2 \Big/ \sum_{k=1}^{K} |A_k|^2 \tag{27}$$

and

$$M_A = \sum_{k=1}^{K} (d_k/c) \ |A_k|^2 \Big/ \sum_{k=1}^{K} |A_k|^2 . \tag{28}$$

Because $J_{\tau\theta} = J_{\theta\tau}$, the product $J_{\tau\theta} J_{\theta\tau}$ in (8) is always non-negative. For given values of $J_{\tau\tau}$ and $J_{\theta\theta}$, and for $J_{\tau\theta} J_{\theta\tau} \geq 0$, (8) indicates that the best performance is obtained when

$$J_{\tau\theta} J_{\theta\tau} = 0 . \tag{29}$$

According to (24c) and (28), this condition is obtained in WGN when the array is symmetric about its midpoint, i.e., when

$$\begin{aligned} &d_2 = -d_1, \ d_4 = -d_3, \ \ldots \\ &|A_2|^2 = |A_1|^2, \ |A_4|^2 = |A_3|^2, \ \ldots \end{aligned} \tag{30}$$

or

$$\begin{aligned} &d_1 = 0, \ d_3 = -d_2, \ d_5 = -d_4, \ \ldots \\ &|A_3|^2 = |A_2|^2, \ |A_5|^2 = |A_4|^2, \ \ldots \ldots \end{aligned} \tag{31}$$

When either (30) or (31) is true, (8) becomes

$$\text{Var} \ (\hat{\tau} - \tau) \geq \left[\text{SNR} \ D_\omega^2 \right]^{-1} \tag{32}$$

$$\text{Var} \ (\hat{\theta} - \theta) \geq \left[\text{SNR} \ D_\omega^2 \ D_A^2 \cos^2\theta \right]^{-1} . \tag{33}$$

Equality in (32) and (33) is asymptotically obtained for a large number of measurements, if a ML estimate is used in WGN (no clutter), and there is accurate prior knowledge of target location.

What, exactly, is meant by "accurate prior knowledge of target location"? How accurate is "accurate"? Does the required accuracy of prior knowledge change when D_ω^2 and/or D_A^2 are increased in (32) and (33)? These questions are often left unanswered in the derivation of parameter estimation methods that are based upon CR bounds, or the problem is side-stepped by assuming that the estimates are consistent and unbiased. It will become apparent, however, that ambiguity analysis provides straightforward answers to these questions.

The bounds in (32) and (33) can be minimized by using two elements at opposite ends of the array and a narrowband signal with the highest allowable frequency. This observation follows easily from the inequalities

$$\int_{-W}^{W} \omega^2 \, |E(\omega)|^2 \, d\omega \le W^2 \int_{-W}^{W} |E(\omega)|^2 \, d\omega \tag{34}$$

$$\sum_{k=1}^{K} d_k^2 \, |A_k|^2 \le \max_k (d_k^2) \sum_{k=1}^{K} |A_k|^2 \tag{35}$$

which become equalities when the signal energy is concentrated at $\pm W$ and only two array elements with the largest d_k-value are used. These solutions, however, have undesirable ambiguity properties, as shown below. A ML processor should be evaluated not only by CR bounds but also by ambiguity function analysis.

Although significant caveats exist for quantitative analysis of (32) and (33), the bounds are qualitatively significant because they illustrate a basic interdependence between signal (temporal) design and array (spatial) design. This interdependence will become even more apparent when ambiguity functions are considered.

The range-angle ambiguity function for targets in the far field of a linear array is obtained by substituting (23) into (13),

$$\chi(\tau, \tau_H, \theta, \theta_H) = \sum_{k=1}^{K} |A_k|^2 \, R\left[\tau - \tau_H + (d_k/c)(\sin\theta - \sin\theta_H)\right]$$

$$= \chi(\tau - \tau_H, \sin\theta - \sin\theta_H) . \qquad (36)$$

If θ and θ_H are less than 30°,

$$\chi(\tau, \tau_H, \theta, \theta_H) \approx \sum_{k=1}^{K} |A_k|^2 \, R\left[\tau - \tau_H + (d_k/c)(\theta - \theta_H)\right]$$

$$= \chi(\Delta\tau, \Delta\theta) . \qquad (37)$$

When the angle hypothesis is correct, we have $\theta_H = \theta$ or $\Delta\theta = 0$, and (36) is proportional to $R(\Delta\tau)$, the echo autocorrelation function. Additional array elements do not affect the structure of $\chi(\Delta\tau, 0)$, and this structure includes many undesirable sidelobes when the signal is narrowband. Figure 2 shows $\chi(\Delta\tau, \Delta\theta)$ for a narrowband pulse and with two hydrophones, i.e., for the "optimum" system design that is obtained from CR bounds as in (34) and (35).

For a single target in a clutter-free environment, Figure 2 indicates that an accurate position estimate can be obtained only if prior knowledge restricts the search area to the central lobe of the ambiguity function. The central lobe becomes more narrow as the signal frequency and the distance between hydrophones increase, so a more accurate estimate implicitly requires better prior knowledge of the estimated parameters. Under clutter-free conditions, one might then expect the two-hydrophone, high frequency system to

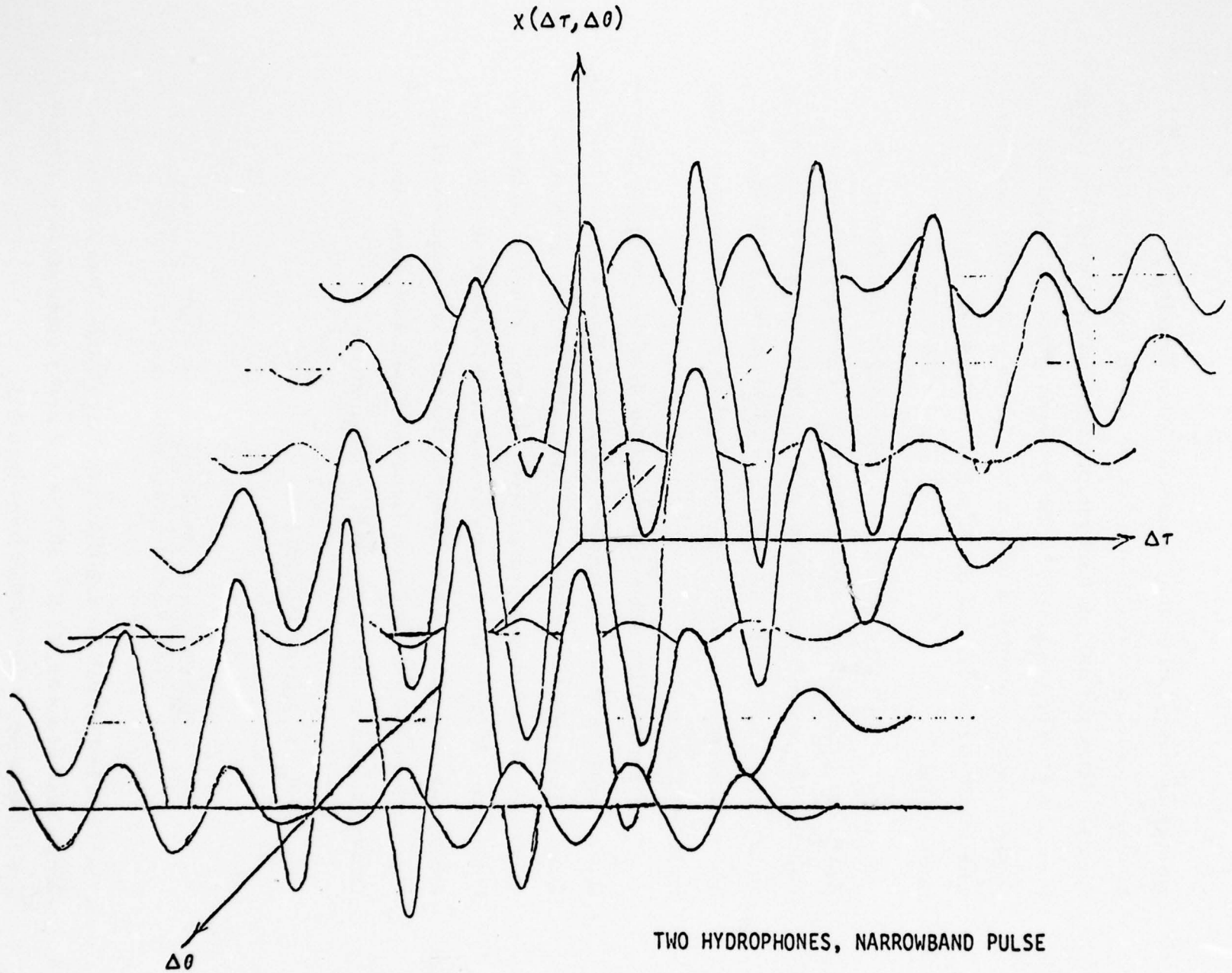

Figure 2. Range-angle ambiguity function for sonar.

emerge as the solution of a sequential beam forming procedure.[16] Ironically, such a final result would be a poor starting point for an adaptive beam former, if the system begins without prior knowledge of τ and θ. The optimality of the two hydrophone configuration depends upon accumulated information (prior probability densities with small variance), and the result is useless without this information.

Far field range ambiguities depend upon the behavior of $R(\Delta\tau)$, the echo autocorrelation function. $R(\Delta\tau)$ becomes more impulse-like when the bandwidth of the echo is increased, and range ambiguities can be reduced by using a wideband signal. In the two hydrophone case, the effect of switching to a wideband signal is illustrated in Figure 3.

Figure 3 illustrates a decomposition of the ambiguity function into a sequence of shifted autocorrelation functions when $\Delta\theta$ becomes large. This effect is predicted by (37). The width of each autocorrelation function is approximately $1/B$ sec, where B is the echo bandwidth. If $(d_k/c)\,\Delta\theta$ is greater than $1/B$ for all k in (37), then a constant-$\Delta\theta$ profile of the ambiguity function is a sequence of K nonoverlapping autocorrelation functions, each with amplitude $|A_k|^2$. Decomposition occurs when $|\Delta\theta| > \Delta\theta_0$, where

$$\Delta\theta_0 = (c/B) \,/\, \min_k (d_k) \qquad (38)$$

$$= \frac{\text{spatial width of echo autocorrelation function}}{\text{minimum distance between hydrophones}} \,.$$

The ratio in (38) can be small if very large bandwidths are used. In the case of sonar, if B = 50 kHz and array elements are 1 meter apart, then $\Delta\theta_0 = .03$ radian (less than 2°).

$$X(\Delta\tau, \Delta\theta) = |A_1|^2 \left\{ R\left[\Delta\tau + (d_1/c)\Delta\theta\right] + R\left[\Delta\tau - (d_1/c)\Delta\theta\right] \right\}$$

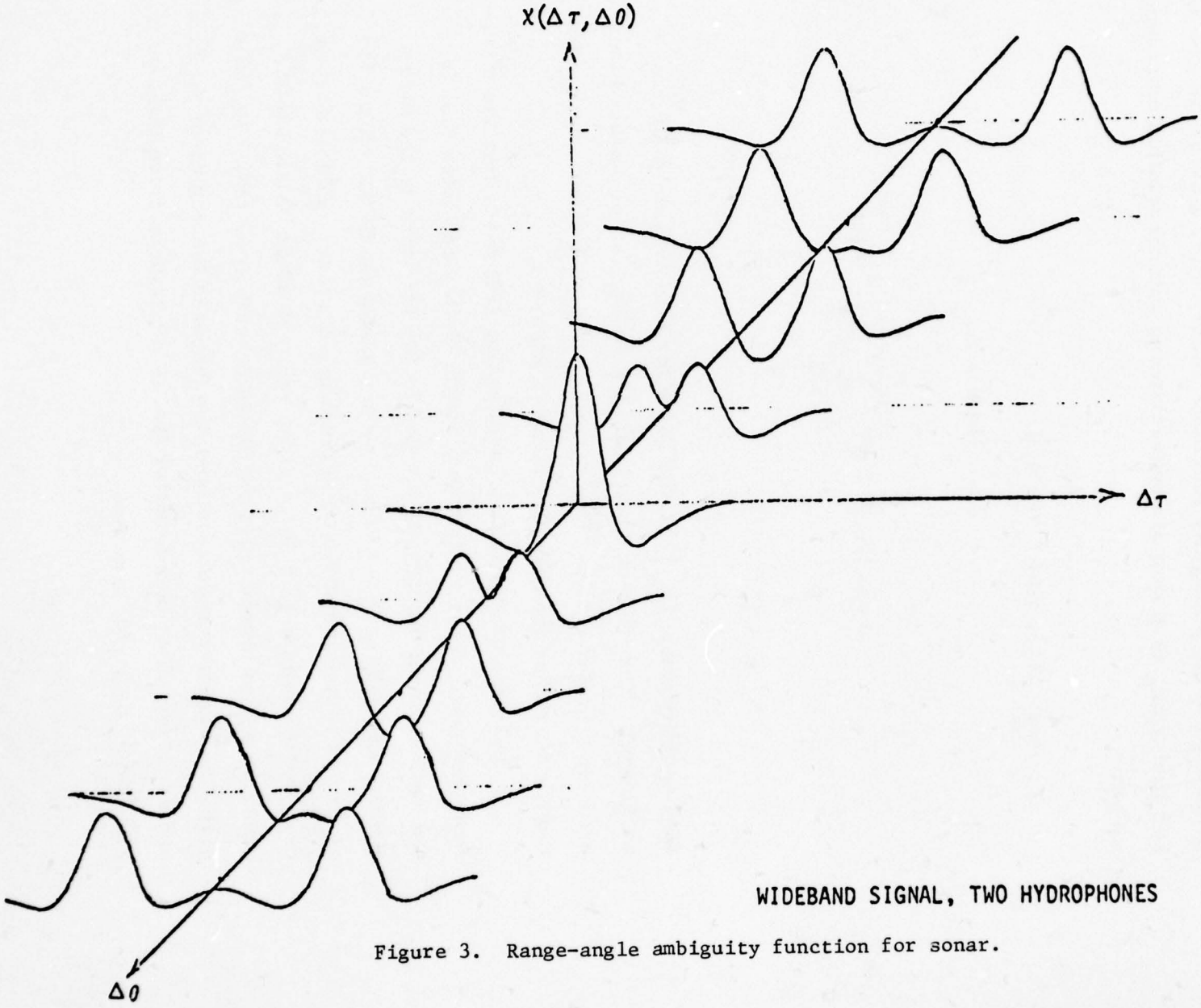

Figure 3. Range-angle ambiguity function for sonar.

For $|\Delta\theta| > \Delta\theta_0$, it is easy to obtain some fundamental properties of the ambiguity function. Since $\chi(\Delta\tau, \Delta\theta)$ for $\Delta\theta$ constant and $|\Delta\theta| > \Delta\theta_0$ is a sum of nonoverlapping autocorrelation functions, we have

$$\max_{\Delta\tau} \chi(\Delta\tau, \Delta\theta) / \chi(0, 0) \Big|_{|\Delta\theta| > \Delta\theta_0}$$

$$= \max_{k} |A_k|^2 R(0) \Big/ \sum_{k=1}^{K} |A_k|^2 R(0) \qquad (39)$$

$$\geq 1/K$$

with equality when $|A_k|^2$ is the same for all k-values (uniform weighting). The sidelobe level for $|\Delta\theta| > \Delta\theta_0$ can be reduced only by using a larger array. For example, Figure 4 shows $\chi(\Delta\tau, \Delta\theta)$ for K = 5, rather than for K = 2, as in Figure 3.

In terms of signal-to-clutter ratio, (39) describes the maximum response of the system to a single clutter reflector that is $\Delta\theta$ radians from the target, divided by the response to the target itself. Eq. (39) is thus a measure of worst-case SCR, where the clutter is restricted to a single point in τ,θ space. For uniformly distributed clutter, SCR for a given value of $\Delta\theta$ is related to the effective beamwidth of the system, as described by (20). Eq. (20) gives the effective angular attenuation between the center of the beam and uniformly distributed clutter that is $\Delta\theta$ radians from the center. For $|\Delta\theta| > \Delta\theta_0$, (20) becomes

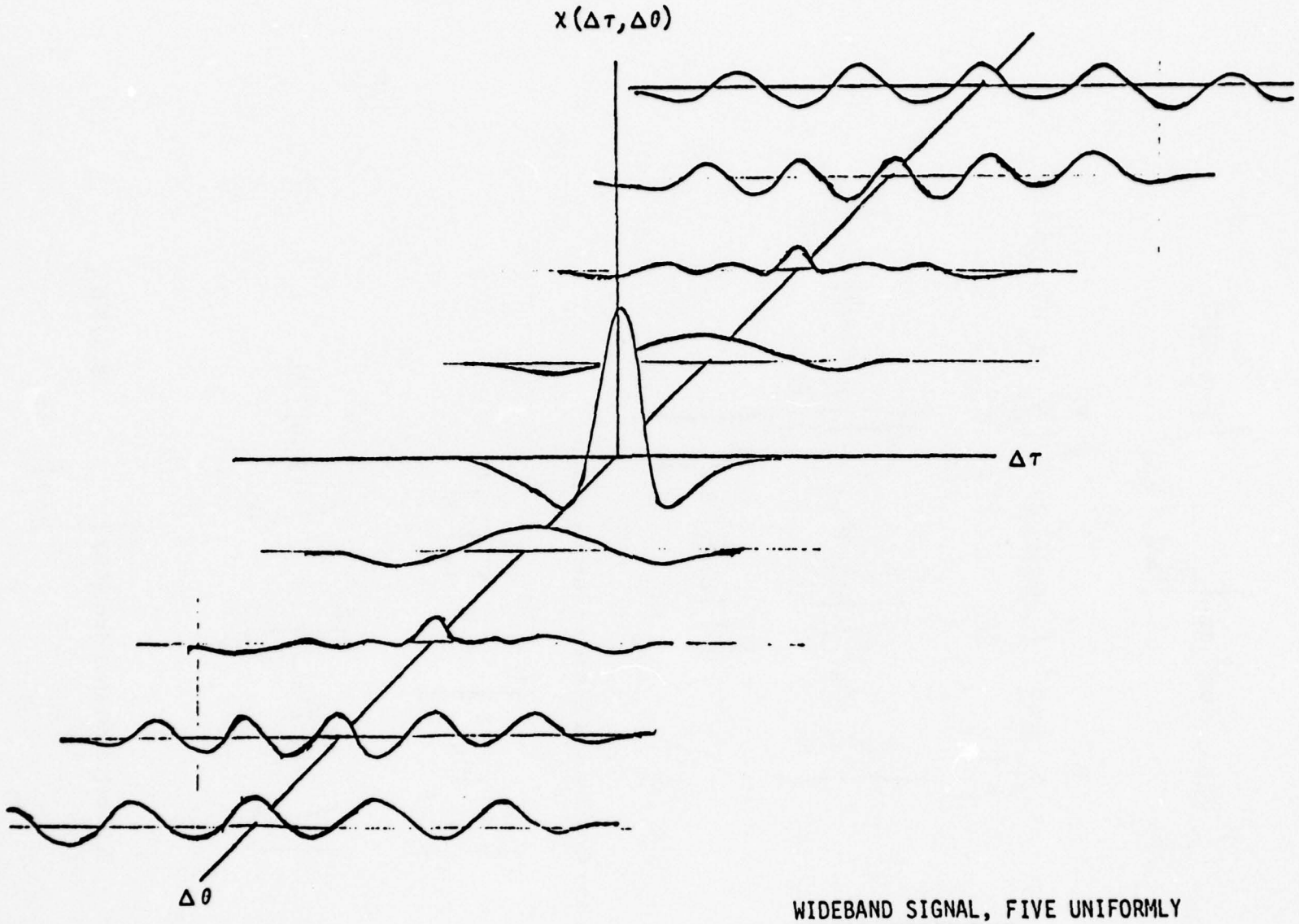

Figure 4. Range-angle ambiguity function for sonar.

$$\int_{-\infty}^{\infty} |\chi(\Delta\tau, \Delta\theta)|^2 \, d\Delta\tau \Bigg|_{|\Delta\theta| > \Delta\theta_0} \Bigg/ |\chi(0,0)|^2$$

$$= \sum_{k=1}^{K} |A_k|^4 \int_{-\infty}^{\infty} |R(\tau)|^2 \, d\tau \Bigg/ \left| \sum_{k=1}^{K} |A_k|^2 R(0) \right|^2$$

$$= \left\{ \sum_{k=1}^{K} |A_k|^4 \Big/ \left[\sum_{k=1}^{K} |A_k|^2 \right]^2 \right\} \left\{ \int_B |E(\omega)|^4 \, d\omega \Big/ \left[\int_B |E(\omega)|^2 \, d\omega \right]^2 \right\}.$$

By the Cauchy and Schwarz inequalities,

$$\left[\sum_{k=1}^{K} |A_k|^2 \right]^2 \leq K \sum_{k=1}^{K} |A_k|^4$$

$$\left[\int_B |E(\omega)|^2 \, d\omega \right]^2 \leq B \int_B |E(\omega)|^4 \, d\omega \, , \tag{40}$$

and

$$\text{Effective attenuation } (\Delta\theta) \Big|_{|\Delta\theta| > \Delta\theta_0} \geq 1/KB \, , \tag{41}$$

with equality when $|A_k|^2$ = constant (uniform weighting in space) and when $|E(\omega)|^2$ = constant over B (uniform weighting in frequency). These equality conditions are the converse of the equality conditions for (34) and (35), which minimize CR bounds by using the ultimate in non-uniform weighting.

For uniformly distributed clutter, the maximum sidelobe level in (39) is not as relevant as the effective attenuation measure in (20) and (41). In order to produce a small effective beamwidth for uniformly distributed clutter, the product KB should be large, and system performance depends equally upon bandwidth and array size. For a given array size, clutter suppression performance can be improved by increasing the bandwidth of the system.

A more general measure of signal-to-clutter ratio is the normalized ambiguity volume in (18) and (19). It is shown in the Appendix that, when $|E(\omega)|^2$ is constant over a bandwidth B,

$$SCR > B/(2\pi)^2 . \tag{42}$$

For uniformly distributed clutter, SCR increases with bandwidth.

An upper bound can be obtained for a two element system which uses a maximum wavelength λ and a bandwidth B such that

$\lambda \leq$ the distance between receiving elements

$B \geq$ one octave.

These conditions hold for many animal sonar systems, e.g., the bottlenosed dolphin (Tursiops truncatus) and the large brown bat (Eptesicus fuscus). For these animals,

$$SCR \leq 2B \tag{43}$$

when clutter is uniformly distributed. Many animal echolocation systems have apparently compensated for their restricted array size by using large bandwidths.

In summary, analysis of the linear array, far field case has demonstrated that optimization on the basis of CR bounds alone is not a desirable procedure unless the environment is clutter-free and there is good prior knowledge of the estimated parameters. The required accuracy of the prior knowledge can be deduced from an appropriate ambiguity function. Qualitative interpretation of CR bounds yields important insight into the fundamental trade-offs between signal and array parameters. These trade-offs can be further investigated by computing bounds on signal-to-clutter ratio, using the range-angle ambiguity function. For uniformly distributed clutter, these bounds depend upon bandwidth alone or upon the product of bandwidth and array size. Array size, independent of bandwidth, becomes important when the clutter consists of a single reflector with particular values of τ and θ.

3.2.5 Linear Array, Near Field

For synthetic aperture systems and for some diagnostic ultrasound applications, targets are often in the near field of the array. The elements of the Fisher information matrix are in this case obtained by substituting (27) into (10). The results are

$$J_{\tau\tau} = \text{SNR}\, D_\omega^2 \sum_{k=1}^{K} \alpha_k^2 |A_k|^2 \Big/ \sum_{k=1}^{K} |A_k|^2 \tag{44a}$$

$$J_{\theta\theta} = \text{SNR}\, D_\omega^2 \cos^2\theta \sum_{k=1}^{K} \beta_k^2 (d_k/c)^2 |A_k|^2 \Big/ \sum_{k=1}^{K} |A_k|^2 \tag{44b}$$

$$J_{\tau\theta}\, J_{\theta r} = \left[\text{SNR}\, D_\omega^2 \cos\theta \sum_{k=1}^{K} \alpha_k \beta_k (d_k/c) \left|A_k\right|^2 \Big/ \sum_{k=1}^{K} \left|A_k\right|^2 \right]^2 \qquad (44c)$$

where SNR and D_ω^2 were defined in (25) and (26) and

$$\alpha_k = \frac{(d_k/c) \sin\theta + \tau}{\tau_k}$$

$$= \frac{\text{approximate far field delay to } k^{th} \text{ element}}{\text{actual delay to } k^{th} \text{ element}} \qquad (45a)$$

$$\beta_k = \tau/\tau_k = \frac{\text{delay to center of array}}{\text{delay to } k^{th} \text{ element}} \quad . \qquad (45b)$$

The expression for $J_{\tau\tau}$ indicates that the array configuration is important for near-field range estimation, a condition that did not exist for far field measurements. As in the far field case, $J_{\theta\theta}$ depends upon both temporal and spatial parameters. If the gains A_k are to be adjusted so as to maximize $J_{\tau\tau}$ and $J_{\theta\theta}$, the optimum weights will depend upon target position. This observation suggests that the gains A_k are no longer decoupled from the position hypothesis τ_H, θ_H, and the gains should change as the environment is scanned. From (45), the element that is closest to the hypothesized target position should have the largest gain. The expression for $J_{\tau\theta}\, J_{\theta\tau}$ indicates that the elimination of range-angle error coupling is more difficult to accomplish in the near field case. This difficulty arises

because differences in the near-field delays τ_k depend upon range as well as angle.

The expression for the near-field ambiguity function can be simplified if τ_k in (27) can be written

$$\tau_k \approx \tau\left\{1 + (1/2)\left[(d_k/c\tau)^2 + 2(d_k/c\tau)\sin\theta\right]\right\} \quad . \tag{46}$$

If the term in square brackets is less than unity, the error in the above approximation is less than 6.4%. We are thus assuming that the distance from the target to the center of the array is larger than the array itself. Substituting (46) into (13),

$$\chi(\tau, \tau_H, \theta, \theta_H) = \sum_{k=1}^{K} |A_k|^2 \; R\left[s_k \Delta\tau + (d_k/c)(\sin\theta - \sin\theta_H)\right] \tag{47}$$

where

$$s_k = 1 - \left[(d_k/c)^2 / (2\tau\tau_H)\right] . \tag{48}$$

The sum in (47) can have an effect that is similar to broadening the bandwidth. When $\theta = \theta_H$, the near-field ambiguity function depends upon a superposition of weighted autocorrelation functions, where each autocorrelation function is scaled by a factor s_k. If the echo autocorrelation function has sidelobes (local maxima at $\Delta\tau \neq 0$), the sum of scaled functions can have a smaller sidelobe level than a sum of unscaled functions, since the maxima for the scaled functions at $\Delta\tau \neq 0$ occur at different locations for different scale factors, s_k. We therefore suspect that the range resolution capabilities of near field systems (e.g., synthetic aperture) will often be better than we would predict from the signal autocorrelation function.

When the distance from the target to the array is smaller than the size of the array itself, the best way to obtain a picture of the range-angle ambiguity function is probably to evaluate (13) by means of a computer. A function of τ_H, θ_H can be displayed for any particular values of τ and θ. The effect of sensor positions, gains, and signal bandwidth upon ambiguity volume can then be empirically determined. If ambiguity volume is used as a measure of system performance (SCR), then the optimum signal/array design can be obtained by gradient techniques.[47]

3.2.6 Direction-Dependent Signals and Array Elements

The effect of transmitting an angle-dependent signal is to replace $|E(\omega)|^2$ in (13) with $E(\omega, \theta)\, E^*(\omega, \theta_H)$. If the inverse Fourier transform of $E(\omega, \theta)\, E^*(\omega, \theta_H)$ has small maximum amplitude for $\theta_H \neq \theta$, the ambiguity function will be rapidly attenuated for $\Delta\theta \neq 0$.

The most common method of achieving direction dependence is through the use of a narrow physical beamwidth. Other methods include the use of a frequency-steered array, a dispersive lens (for sonar), and movement of the array with respect to the environment, so that an angle-dependent Doppler history is obtained from each target. The latter method is employed in synthetic aperture systems.[17,18] Angle-dependent Doppler shifts could also be used in ultrasonic blood flow measurements, where movement of the target would replace movement of the array.

Direction-dependent array elements can also increase angle resolution.[11] To include the effect of a direction dependent transfer function, the gain A_k in (2) is replaced by $A_k(\theta)$. More generally, we can take account of the temporal impulse response of the element

by using $A_k(\theta, \omega)$. The quantity $|A_k|^2$ in (13) is then replaced by $A_k(\theta, \omega)\, A_k^*(\theta_H, \omega)$. The effect is again to reduce the level of $\chi(\Delta_T, \Delta\theta)$ for nonzero $\Delta\theta$.

A direction-dependent receiving element that makes use of multiple reflections, as in the human pinna,[19] imposes a direction-dependent convolutional code upon received wideband waveforms. If the receiver can decode the resulting signal, good angle resolution can be obtained with a very compact physical array. The trade-off here is between array size and processor complexity.

It is likely that animal echolocation systems exploit direction dependence of transmitted and received signals.[11] A transmitted dolphin echolocation pulse has different structure when it is observed at different angles relative to the animal,[20,21] and the external ears of many bats are capable of imposing a direction-dependent code upon received signals.

3.2.7 Extended Targets and System Identification

The formulation in (11) to (13) can produce a generalized ambiguity function[13] for any ML estimation problem, and it would seem that the ambiguity function should not be restricted to radar/sonar applications. Ambiguity analysis should be especially beneficial for system identification, where CR analysis has already been applied to the design of probing signals.[22-24] The shortcomings of signal derivations that are based upon CR bounds alone have already been discussed. It remains to demonstrate the utility of ambiguity analysis for system identification. The advantages of ambiguity analysis should be obvious if we can find a system identification problem that involves radar/sonar measurements. Parameterization of extended targets is ideal for this purpose.

An extended target can sometimes be described as a distribution of point reflectors or highlights in range-angle space. Most diagnostic ultrasound and synthetic aperture imaging systems are based upon such a description. In estimating the position of each highlight, reflections from the other highlights can be regarded as clutter. We have seen that CR bounds, derived under WGN conditions, are not applicable to this situation. An impulse-like ambiguity function, however, will be capable of resolving the target into its separate highlights, or at least of determining the target reflectivity within a small range-angle cell.

An extended target can also be characterized as a distributed parameter system. The impulse response is a function of time (range) for a given angle, and the impulse response changes with angle. The system is to be parameterized by the locations (i.e., the τ, θ values) of large local maxima in the impulse response (i.e., the highlights). Each of these position parameters is to be estimated in the presence of noise and spurious signal components (clutter) that are part of the system's response to the probing signal.

The system identification problem for an extended target is thus equivalent to the estimation of a sequence of τ, θ values in clutter. The ambiguity function is a valuable aid in the design of signals and filters that can perform the required identification. Exclusive use of CR bounds for design of the probing signal for this identification problem can result in an ambiguity function with large volume or large sidelobes, and undesirable interaction between parameter estimates will result. The concept of resolution in radar/sonar performance translates into parameter separability or increased observability in control theory. In a system identification context, the volume of the ambiguity function is a measure of the extent to which each parameter estimate is unaffected by the remaining system parameters.

3.2.8 Conclusion

A range-angle ambiguity function can be used to predict signal-to-interference ratios for high-resolution radar/sonar systems. The expected clutter response will often depend upon the volume under the sidelobes of the ambiguity function, rather than the height of these sidelobes. For a given array size, the sidelobes are made "thinner" by using a wideband signal, the volume is thus reduced, and signal-to-interference ratio is increased.

Direction-dependent, wideband echoes can result in an impulse-like range-angle ambiguity function. In synthetic aperture systems, the direction dependence is obtained by moving the radar or sonar relative to the environment. Other methods that do not depend upon movement can perhaps be used to increase the rate at which a given area can be mapped. For example, one can use an angle-dependent pulse with large time-bandwidth product, and this signal could be transmitted in all directions simultaneously.

It would seem that the range-angle ambiguity function is a radar/sonar counterpart of the point spread function that is used to define visual acuity. It is therefore a useful concept for sonar systems that are attempting to "see with sound." The trade-off between bandwidth and array size, which has been obtained from properties of the range-angle ambiguity function, would seem to be important for echolocating animals that use wideband signals.

Cramér-Rao bounds are helpful indicators of qualitative interdependencies between temporal and spatial parameters. The exclusive use of CR bounds for signal and array synthesis, however, can lead to results which are only optimum in the immediate neighborhood of a particular position, i.e., with accurate prior knowledge

of τ and θ. The global behavior of the maximum likelihood estimate is portrayed by the ambiguity function, which provides a more reliable functional for synthesis of signals and array configurations. This observation can be generalized to any parameter estimation problem, and it appears to be especially relevant to the design of probing signals for system identification.

Multiparameter space-time ambiguity analysis can be used to determine the best array locations for passive sonar systems, and the approach is also applicable to signal design and transmitter placement for radio navigation.

In many cases, ambiguity volume depends upon the properties of the estimation device, and a small volume is indicative of parameter separability. Computer minimization of the volume of a multidimensional ambiguity function should result in an optimum estimating device, e.g., an optimum probing signal for system identification.

3.2.9 References for Section 3.2

1. H. Cramér, Mathematical Methods of Statistics. Princeton: Princeton Univ. Press, 1945.

2. H. L. Van Trees, Detection, Estimation, and Modulation Theory, Part I. New York: Wiley, 1968.

3. P. M. Woodward, Probability and Information Theory with Applications to Radar. Oxford: Pergamon, 1964.

4. C. E. Cook and M. Bernfeld, Radar Signals. New York: Academic, 1967.

5. D. F. DeLong, Jr., and E. M. Hofstetter, "On the design of optimum radar waveforms for clutter rejection," IEEE Trans. on Inform. Theory, vol. IT-13, pp. 454-463, 1967.

6. W. D. Rummler, "Clutter suppression by complex weighting of coherent pulse trains," IEEE Trans. on Aerospace and Electronic Systems, vol. AES-2, pp. 689-699, 1966.

7. E. N. Fowle, E. J. Kelly, and J. A. Sheehan, "Radar system performance in a dense-target environment," 1961 IRE Conv. Rec. pt. 4, pp. 136-145, 1961.

8. C. A. Stutt and L. J. Spafford, "A 'best' mismatched filter response for radar clutter discrimination," IEEE Trans. on Inform. Theory, vol. IT-14, pp. 280-287, 1968.

9. H. L. Van Trees, Detection, Estimation, and Modulation Theory, Part III. New York: Wiley, 1971.

10. R. A. Altes, "Suppression of radar clutter and multipath effects for wide-band signals," IEEE Trans. Inform. Theory, vol. IT-17, pp. 344-346, 1971.

11. R. A. Altes, "Angle estimation and binaural processing in animal echolocation," J. Acous. Soc. Amer., vol. 63, pp. 155-173, 1978.

12. L. E. Brennan and J. S. Reed, "Theory of adaptive radar," IEEE Trans. on Aerospace and Electronic Systems, vol. AES-9, pp. 237-252, 1973.

13. H. Urkowitz, C. A. Hauer, and J. F. Koval, "Generalized resolution in radar systems," Proc. IRE, vol. 50, pp. 2093-2105, 1962.

14. R. J. Purdy and G. R. Cooper, "A note on the volume of generalized ambiguity functions," IEEE Trans. on Inform. Theory, vol. 14, pp. 153-154, 1968.

15. R. A. Altes, "Some invariance properties of the wide-band ambiguity function," J. Acous. Soc. Amer., vol. 53, pp. 1154-1160, 1973.

16. L. W. Nolte and W. S. Hodgkiss, "Directivity or Adaptivity?" Eascon '75, pp. (35-A) - (35-H), 1975.

17. W. M. Brown and L. J. Porcello, "An introduction to synthetic-aperture radar," IEEE Spectrum, pp. 52-62, Sept. 1979.

18. L. J. Cutrona, "Comparison of sonar system performance achievable using synthetic-aperture techniques with the performance achievable by more conventional means," J. Acous. Soc. Am., Vol. 58, pp. 336-348, 1975.

19. D. W. Batteau, "Role of the pinna in localization: theoretical and physiological consequences," in Hearing Mechanisms in Vertebrates, De Reuck and Knight, eds. London: Churchill, 1968.

20. W. E. Evans, "Echolocation by marine delphinids and one species of fresh-water dolphin," J. Acous. Soc. Am., vol. 54, pp. 191-199, 1973.

21. M. S. Livshits, "Some properties of the dolphin hydrolocator from the viewpoint of a correlation hypothesis," Biofizika, vol. 19, pp. 916-920, 1974. Also JPRS 64329.

22. R. K. Mehra, "Optimal input signals for parameter estimation in dynamic systems-survey and new results," IEEE Trans. on Automatic Control, vol. AC-19, pp. 753-768, 1974.

23. G. D. Swanson, "Biological signal conditioning for system identification," Proc. IEEE, vol. 65, pp. 735-740, 1977.

24. M. Aoki and R. M. Staley, "On input signal synthesis in parameter identification," Automatica, vol. 6, pp. 431-440, 1970.

25. M. Abramowitz and I. A. Stegun, eds., Handbook of Mathematical Functions, NBS Applied Math. Series 55, Washington: U. S. Govt. Printing Office, 1964.

26. D. R. Griffin, Listening in the Dark. New Haven: Yale Univ. Press, 1958.

27. D. E. Vakman, Sophisticated Signals and the Uncertainty Principle in Radar. New York: Springer-Verlag, 1968.

28. H. Maxim, "The sixth sense of the bat. Sir Hiram's contention. The possible prevention of sea collisions." Scientific Amer., Suppl., pp. 148-150, Sept. 7, 1912.

29. F. A. Webster, "Interception performance of echolocating bats in the presence of interference," in Animal Sonar Systems, vol. 1, R. G. Busnel, ed. Jouy-en-Josas: Laboratoire de Physiologie Acoustique, 1966.

30. D. R. Griffin, "Discriminative echolocation by bats," in Animal Sonar Systems. See ref. 29.

31. R. A. Altes and W. D. Reese, "Doppler tolerant classification of distributed targets--a bionic sonar," IEEE Trans. on Aerosp. and Electron. Sys., vol. AES-11, pp. 708-723, 1975.

32. R. A. Altes, "Sonar for generalized target description and its similarity to animal echolocation systems," J. Acous. Soc. Amer., vol. 59, pp. 97-105, 1976.

33. D. P. Skinner, R. A. Altes, and J. D. Jones, "Broadband target classification using a bionic sonar," J. Acous. Soc. Amer., vol. 62, pp. 1239-1246, 1977.

34. G. L. Turin, "On the estimation in the presence of noise of the impulse response of a random, linear filter," IRE Trans. Inform. Theory, vol. IT-3, pp. 5-10, 1957.

35. R. A. Altes, "Estimation of sonar target transfer functions in the presence of clutter and noise," J. Acous. Soc. Amer., vol. 61, 1371-1374, 1977.

36. R. A. Altes, "Optimum waveforms for sonar velocity discriminations," Proc. IEEE (lettr.), vol. 59, 1615-1617, 1971.

37. R. A. Altes and D. P. Skinner, "Sonar velocity resolution with a linear-period-modulated pulse," J. Acous. Soc. Am., vol. 61, pp. 1019-1030, 1977.

38. A. W. Rihaczek, Principles of High-Resolution Radar. New York: McGraw-Hill, 1969.

39. R. A. Altes and E. L. Titlebaum, "Bat signals as optimally Doppler tolerant waveforms," J. Acous. Soc. Am., vol. 48, pp. 1014-1020, 1970.

40. R. A. Altes and E. L. Titlebaum, "Graphical derivations of radar, sonar, and communication signals," IEEE Trans. on Aerosp. and Electron. Sys., vol. AES-11, pp. 38-44, 1975.

41. M. I. Skolnik, "Sea Echo," Chapter 26 in Radar Handbook, M. I. Skolnik (ed.), New York: McGraw-Hill, 1970.

42. D. K. Barton, "Radar measurement accuracy in log-normal clutter," Eascon. 1971, pp. 246-251.

43. A. Papoulis, "Narrow-band systems and Gaussianity," IEEE Trans. Inform. Theory, vol. IT-18, pp. 20-27, 1972.

44. W. S. Hodgkiss and L. W. Nolte, "Covariance between Fourier coefficients representing the time waveforms observed from an array of sensors," J. Acous. Soc. Am., vol. 59, pp. 582-590, 1976.

45. E. J. Kelly and R. P. Wishner, "Matched filter theory for high-velocity, accelerating targets," IEEE Trans. on Mil. Electronics, vol. MIL-9, pp. 56-69, 1965.

46. S. S. Haykin, ed. Detection and Estimation, Applications to Radar. Benchmark papers in Electrical Engineering and Computer Science, vol. 13, Bowden, Hutchinson, and Ross, 1976.

47. D. G. Luenberger, Optimization by Vector Space Methods. New York, Wiley, 1969, Chapter 10.

3.2.10 Appendix to Section 3.2

Signal to clutter ratio is defined as the ratio P_T/P_C, where

$$P_T = |X(\tau, \tau, \theta, \theta)|^2 \qquad \text{(A-1)}$$

and

$$P_C \propto \int_{-\infty}^{\infty} d\tau_c \int_{-\pi}^{\pi} d\theta_c \; p(\tau_c, \theta_c) \; |X(\tau, \tau_c, \theta, \theta_c)|^2 . \qquad \text{(A-2)}$$

In (A-2), $p(\tau_c, \theta_c)$ is the clutter probability density function or a normalized version of the clutter scattering function, and

$$X(\tau, \tau_c, \theta, \theta_c) = (1/2\pi) \sum_{k=1}^{K} |A_k|^2 \int_{-\infty}^{\infty} |E(\omega)|^2 \exp\left\{j\omega\left[(d_k/c)\right.\right.$$

$$\left.\left.(\sin\theta - \sin\theta_c) + \tau - \tau_c\right]\right\} d\omega$$

$$= X(\tau - \tau_c, \sin\theta - \sin\theta_c) \qquad \text{(A-3)}$$

for a far-field condition.

For uniformly distributed clutter,

$$P_C \equiv (1/2\pi)^2 \sum_{k,\,n} |A_k|^2 \; |A_n|^2 \int_{-\pi}^{\pi} d\theta_c \int_{-\infty}^{\infty} d\tau_c \iint_{-\infty}^{\infty}$$

$$|E(\omega_1)|^2 \; |E(\omega_2)|^2 \; \exp\left\{j\omega_1\left[(d_k/c)\right.\right.$$

$$\left.\left.(\sin\theta - \sin\theta_c) + \tau - \tau_c\right]\right\}$$

$$\exp\left\{-j\omega_2\left[(d_n/c)(\sin\theta - \sin\theta_c) + \tau - \tau_c\right]\right\} d\omega_1\, d\omega_2 . \quad (A-4)$$

Performing the τ_c integration, we have

$$(1/2\pi)\int_{-\infty}^{\infty} \exp\left[-j(\omega_1 - \omega_2)\,\tau_c\right] d\tau_c = \delta(\omega_2 - \omega_1)$$

and

$$P_C = \sum_{k,n} |A_k|^2\, |A_n|^2 \int_{-\infty}^{\infty} |E(\omega)|^4 \exp\left[j(\omega/c)(d_k - d_n)\sin\theta\right] \cdot \left\{(1/2\pi)\int_{-\pi}^{\pi} \exp\left[-j(\omega/c)(d_k - d_n)\sin\theta_c\right] d\theta_c\right\} d\omega \quad . \quad (A-5)$$

The imaginary part of the θ_c-integral is zero, i.e.,

$$-(1/2\pi)\int_{-\pi}^{\pi} \sin\left[(\omega/c)(d_k - d_n)\sin\theta_c\right] d\theta_c \equiv 0$$

because the integrand is an odd function of θ_c and the limits of integration are symmetric about $\theta_c = 0$. The real part of the θ_c integral is[25]

$$(1/\pi)\int_{0}^{\pi} \cos\left[(\omega/c)(d_k - d_n)\sin\theta_c\right] d\theta_c$$

$$= J_0\left[(\omega/c)(d_k - d_n)\right]$$

where $J_0(\cdot)$ is a Bessel function of order zero. It follows that

$$P_C = \sum_{k,n} |A_k|^2 \, |A_n|^2 \int_{-\infty}^{\infty} |E(\omega)|^4 \, J_0\left[(\omega/c)\,(d_k - d_n)\right]$$

$$\exp\left[j(\omega/c)\,(d_k - d_n)\sin\theta\right] \, d\omega \, . \qquad \text{(A-6)}$$

The expected clutter response for uniformly distributed clutter is therefore a function of θ, the angle between a line drawn from the center of the array to the target and a line that is normal to the array. An upper bound on P_C can be obtained by noting that

$$\left| J_0\left[(\omega/c)\,(d_k - d_n)\right] \exp\left[j\,(\omega/c)\,(d_k - d_n)\sin\theta\right] \right| \leq 1 \, ,$$

and therefore

$$P_C \leq \left[\sum_{k=1}^{K} |A_k|^2 \right]^2 \int_{-\infty}^{\infty} |E(\omega)|^4 \, d\omega \, . \qquad \text{(A-7)}$$

From (A-1) and (A-3),

$$P_T = \left[(1/2\pi) \sum_{k=1}^{K} |A_k|^2 \int_{-\infty}^{\infty} |E(\omega)|^2 \, d\omega \right]^2 \qquad \text{(A-8)}$$

and

$$P_T/P_C \geq \left[(1/2\pi) \int_{-\infty}^{\infty} |E(\omega)|^2 \, d\omega \right]^2 \Bigg/ \int_{-\infty}^{\infty} |E(\omega)|^4 \, d\omega \, . \qquad \text{(A-9)}$$

If $|E(\omega)|^2$ is constant over a bandwidth B, then, from (40),

$$P_T/P_C \geq B / (2\pi)^2 . \qquad \text{(A-10)}$$

For uniformly distributed clutter, the lower bound (A-10) on signal-to-clutter ratio will increase as bandwidth increases.

An upper bound for SCR can be obtained when (i) the maximum echo wavelength is less than the minimum distance between hydrophones, and (ii) the echo spectral magnitude is smooth and has at least an octave bandwidth. The first condition means that[25]

$$J_0(x) \approx (2/\pi x)^{\frac{1}{2}} \cos (x - \pi/4)$$

where

$$x = (\omega/c) (d_k - d_n) .$$

The error in the approximation is less than 3.2% for

$$x > 2\pi$$

or

$$\min_{k,n} \left| d_k - d_n \right| > \lambda ,$$

which is condition (i).

The second condition implies that, for $k \neq n$,

$$\left| \int_{-\infty}^{\infty} |E(\omega)|^4 \, J_0 \left[(\omega/c) (d_k - d_n) \right] d\omega \right| << \int_{-\infty}^{\infty} |E(\omega)|^4 \, d\omega \qquad \text{(A-11)}$$

because the smooth non-negative function $|E(\omega)|^4$ is multiplied by a periodic function with at least one full oscillation. Substituting (A-11) into (A-6),

$$P_T/P_C\Big|_{\theta=0} \approx \frac{\left[\sum_k |A_k|^2\right]^2 \left[\int_{-\infty}^{\infty} |E(\omega)|^2 \, d\omega\right]^2}{\sum_k |A_k|^4 \int_{-\infty}^{\infty} |E(\omega)|^4 \, d\omega} . \qquad \text{(A-12)}$$

and from (40)

$$P_T/P_C\Big|_{\theta=0} \leq KB . \qquad \text{(A-13)}$$

The approximation in (A-11) must be used carefully, since the sum of the left-hand side over a large number of elements may not be small relative to the right-hand side, even though each term of the sum is small. This reservation is inconsequential for studies of animal echolocation, where K = 2. The two conditions that lead to (A-13) are satisfied by many wide-band animal echolocation systems. For the Atlantic bottlenose dolphin, Tursiops truncatus, echolocation pulses cover a frequency range between about 20 and 150 kHz.[20] The maximum wavelength in water is 7.5 cm, which is shorter than the distance between the ears. The large brown bat, Eptesicus fuscus, has a cruising pulse that covers the frequency range between about 25 and 65 kHz.[26] The maximum wavelength in air is 1.3 cm, which

is again shorter than the distance between the ears. Although many animals are restricted to two array elements, they can obtain good SCR by using very wide bandwidths.

3.3 Measurement of Tangential Velocity and Evasive Maneuvers

3.3.1 Introduction to Section 3.3

The utilization of evasive maneuvers by moths is well documented for bat echolocation.[1] Noctuid moths that are 10 to 100 feet away from a bat generally fly away from the sound source, and those that are close enough to be tracked display erratic flight patterns. Tangential motion (i.e., motion perpendicular to the direction of propagation) is an optimum maneuver for the differential game known as the homicidal chauffeur problem.[2]

Although evasive action by fish is less well documented, the use of a sudden tangential motion to escape a threat at close range is familiar to any skin diver or aquarium hobbyist. If a dolphin is to catch prey at night or in very turbid water, high survival value would be attached to the detection of tangential motion, i.e., motion that is normal to the dolphin's own velocity vector, at close range.

What is the best way to measure tangential velocity, and how might it be measured in animal sensory systems? It would appear that a maximum likelihood estimate of cross-range velocity can be obtained by frequency shifting (or time scaling) the input to one ear and correlating this shifted (or scaled) signal with the input to the other ear. Maximum correlator response will occur when the Doppler shift has been correctly hypothesized. This frequency shift and cross correlation is analogous to the time shift and cross correlation that has been suggested by Licklider[3] and Sayers and Cherry[4] as a model for binaural interaction. An equivalent operation can also be implemented by the equalization-cancellation model[5] that has been proposed by Durlach.[6]

If we were to simultaneously estimate interaural delay (for angle measurement) and interaural Doppler shift (for tangential velocity measurement) then the output $u_1(t)$ of one ear should be frequency shifted and delayed, and then correlated with the output

$u_2(t)$ of the second ear. The correlator response is a function of the frequency shift, ϕ, and the delay, τ. This response is the cross-ambiguity function of the echo, $\chi_{u_1u_2}(\tau, \phi)$.

There are some interesting theoretical implications to the conjecture that the cross-ambiguity function $\chi_{u_1u_2}(\tau, \phi)$ is formed by the auditory system. It can be shown[8] that the auto-ambiguity function of the input to each ear can be estimated from the spectrogram of the signal (i.e., the output of a model for the peripheral auditory system). Given the two resulting auto-ambiguity functions $\chi_{u_1u_1}(\tau, \phi)$ and $\chi_{u_2u_2}(\tau, \phi)$, we would like to construct the magnitude-squared cross-ambiguity function $|\chi_{u_1u_2}(\tau, \phi)|^2$. In man-made systems, this construction can be accomplished by making use of Stutt's Fourier transform theorem:[9]

$$|\chi_{u_1u_2}(-\tau, \phi)|^2 = F^{-1}\left[\chi_{u_1u_1}(t, f)\chi^*_{u_2u_2}(t, f); \tau, \phi\right]$$

$$= \int\int_{-\infty}^{\infty} \chi_{u_1u_1}(t,f)\chi^*_{u_2u_2}(t,f)\, e^{j2\pi(\phi t + \tau f)}\, dt\, df$$

where the operation on the right-hand side is a two-dimensional inverse Fourier transform of the product of the two auto-ambiguity functions.

Using Stutt's Theorem, it is straightforward to form a cross-ambiguity function for simultaneous estimation of interaural delay (angle) and interaural frequency shift (tangential velocity or evasive maneuver).

The cross-ambiguity function predicts the behavior of a system that uses cross-correlation to measure interaural velocity difference. Such a prediction can be checked against the performance of an animal in an appropriate discrimination experiment. If performance and prediction are closely matched, then one has support for the hypothesis that tangential velocity is estimated by a cross-correlation process. A similar approach has been used by Sayers and Cherry,[4] who have shown that a listener's uncertainty about sound direction corresponds to ambiguities in the interaural cross-correlation function. The method has also been used by Simmons to compare bat range resolution performance with the performance of a correlator that is matched to the bat's echolocation signal.[7]

3.3.2 Standard Deviation of a Cross-Range Velocity Estimate

The following calculations demonstrate the feasibility of tangential velocity estimation in animal echolocation.

Consider two transducers that are d meters apart, and that are each r meters from a target (Figure 1).

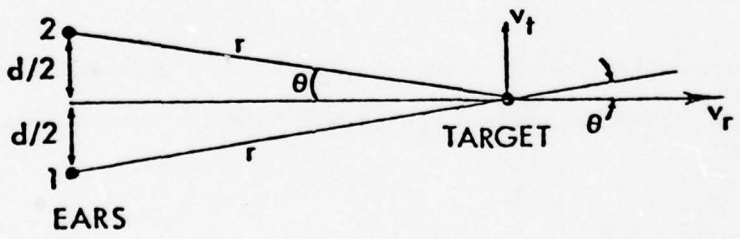

Figure 1.

The target has velocity components v_r and v_t which correspond to radial and tangential velocities, respectively.

The radial velocity at ear #1 is

$$\dot{r}_1 = v_r \cos\theta + v_t \sin\theta \tag{1}$$

and the radial velocity at ear #2 is

$$\dot{r}_2 = v_r \cos\theta - v_t \sin\theta, \tag{2}$$

where

$$\sin\theta = d/2r . \tag{3}$$

From (1) – (2), we have

$$\dot{r}_1 - \dot{r}_2 = 2 v_t \sin\theta . \tag{4}$$

Consider a bat such as Rhinolophus and a moth that is undertaking evasive action with tangential velocity v_t. We assume that it is sufficient for the bat to estimate the direction of the moth's motion, i.e., the sign of v_t. In this case, it is sufficient to require that the uncertainty in measuring v_t is less than $|v_t|$, the magnitude of the tangential velocity component. In other words, we require that

$$\Delta v_t < |v_t| \tag{5}$$

where Δv_t is the standard deviation of the velocity measurement. For a narrowband signal and a white, Gaussian noise background, an optimum velocity estimator has standard deviation[10]

$$\Delta\phi = (\mathrm{SNR})^{-\frac{1}{2}}\, T^{-1} \tag{6}$$

where T is the observation time (the length of the bat's pulse) and SNR is signal energy divided by noise power spectral density (signal to noise ratio). The quantity $\Delta\phi$ in (6) is the uncertainty in Doppler shift ϕ, where

$$\phi = 2 f_o \dot{r}/c \tag{7}$$

and where f_o is the center frequency of the signal, $\dot{r}$ is range rate, and c is the speed of sound. In our case, $\dot{r}$ is either $\dot{r}_1$ or $\dot{r}_2$,

$$f_o \approx 80\ \mathrm{kHz}, \quad \text{and} \quad c \approx 330\ \mathrm{m/s}\ .$$

The uncertainty of v_t is, from (4),

$$\Delta v_t = \Delta(\dot{r}_1 - \dot{r}_2) / 2 \sin\theta \tag{8}$$

where, if the noise processes at ear 1 and ear 2 are independent,

$$\Delta(\dot{r}_1 - \dot{r}_2) = \sqrt{(\Delta\dot{r}_1)^2 + (\Delta\dot{r}_2)^2} = \sqrt{2}\ \Delta\dot{r}_1 \tag{9}$$

and, from (7)

$$\Delta\dot{r}_1 = c\,\Delta\phi / 2 f_o\ . \tag{10}$$

Combining (3) – (10),

$$\Delta v_t = r c / (\sqrt{2\,\mathrm{SNR}}\ T f_o\, d)\ . \tag{11}$$

Suppose that Rhinolophus first detects its prey at r = 4 m. At this range, we assume that SNR = 3 dB. At r = 50 cm, SNR is then greater than 2×8^4, where the acoustic absorption of the air has

been neglected. It follows from (11) that, at $r = 50$ cm and for $d = 2$ cm,

$$\Delta v_t < (13T \times 10^2)^{-1} . \tag{12}$$

An average Rhinolophus cruising pulse is 67 msec long,[11] but the pulses shorten as range decreases. If $T = 2.5$ msec, $\Delta v_t < 0.3$ m/sec. This resolution should be sufficient to determine the direction of most evasive maneuvers.

Wideband, Doppler tolerant signals are used by some FM bats[12] and by cetaceans.[13,14] Such signals can be used for velocity estimates if range rate is measured with more than one echo pulse.

When multiple pulses are used, it would seem that tangential velocity should be estimated by measuring rate of angle change, i.e., difference in estimated target direction for two different echo pulses. One component in an angle measurement is the relative delay between the ears, which is proportional to $r_1 - r_2$. The rate of angle change is then dependent upon measurement of the time derivative of $(r_1 - r_2)$, i.e., upon $\dot{r}_1 - \dot{r}_2$. From (4), $\dot{r}_1 - \dot{r}_2$ can be interpreted as a tangential velocity measure. The uncertainty Δv_t is thus partially indicative of the uncertainty in an angle rate measurement.

For a train of wideband pulses, range rate induces a scaling effect,[15] and the pulse train is stretched or compressed by a factor s, where

$$s \approx 1 + 2\dot{r}/c . \tag{13}$$

The uncertainty in measuring s depends upon the time-bandwidth product TW of the pulse train[16,17]

$$\Delta s = (SNR)^{-\frac{1}{2}} (TW)^{-1} . \qquad (14)$$

From (13) – (14),

$$\Delta \dot{r} = c\,(SNR)^{-\frac{1}{2}} (2TW)^{-1} . \qquad (15)$$

Using (8) – (9), we have

$$\Delta v_t = r c\,(2SNR)^{-\frac{1}{2}} (TW\,d)^{-1} . \qquad (16)$$

Comparison of (16) and (11) shows that center frequency f_o for narrowband measurement of Δv_T is replaced by bandwidth W for wideband measurement with a pulse train. If a new pulse is transmitted shortly after a previous pulse is received, then $T \approx 2Nr/c$, where N is the number of pulses that are used for the velocity estimate, and

$$\Delta v_t = c^2\,(2SNR)^{-\frac{1}{2}} (2NW\,d)^{-1} . \qquad (17)$$

For the FM bat, Natalus mexicanus, we have W ≈ 115 kHz if harmonics are used. If initial detection takes place at SNR = 3 dB and at 4 meters from the bat, then (neglecting energy absorption by the air) the SNR at r = 50 cm is 2×8^4. Again assuming that d = 2 cm, and c = 330 m/s, we have, for r = 50 cm,

$$\Delta v_t = 1/(6N) \text{ m/s} . \qquad (18)$$

Two pulses (N = 2) are thus sufficient to obtain an accurate estimate of tangential velocity for assessment of evasive maneuvers at r = 50 cm.

For the Atlantic bottlenose dolphin, Tursiops truncatus, we have W ≈ 100 kHz, d ≈ 20 cm, and c ≈ 1500 m/s. Detection

distances for the dolphin are larger than for the bat,[18] and we can assume that SNR = 3 dB at least 10 m away from the animal. For r = 1 m, we then have SNR = 2×10^4, and (17) gives

$$\Delta v_t = 1/4N \text{ m/s} \tag{19}$$

for r = 1 m. Two pulses (N = 2) are again sufficient for accurate estimation of tangential velocity for dolphin echolocation.

3.3.3 Experiments to Test Sensitivity to Tangential Velocity in Mammals

The simplest experiment is to test whether an illusion of movement can be caused in a human listener by introducing a time gated sinusoid

$$u_1(t) = \sin (2\pi f_o t) \text{ rect } (t) \tag{20}$$

into one ear and another gated sinusoid of slightly different frequency

$$u_2(t) = \sin [2\pi (f_o + \phi) t] \text{ rect } (t) \tag{21}$$

into the other ear by means of earphones. In (20) – (21), rect (t) is a rectangular on-off function or time gate. The direction of the apparent movement should depend upon the sign of ϕ, and the speed of movement should depend upon its magnitude.

A more complicated experiment is to construct signals that have deliberate velocity ambiguities, such as the sum of the two signals in (20) and (21). It should be theoretically possible to

correlate listener confusion about apparent motion with local peaks in the cross-ambiguity function of the signals that are supplied to each ear.

For echolocating animals, sensitivity to tangential velocity can be tested by using an array of loudspeakers that are placed in a semicircle around the animal, or by mechanically moving a sound source or target on a semicircular trajectory. If the animal is trained to signify the direction of movement, then the limits of its measurement ability can be tested for very slow motion, and resolution can be tested by using two sound sources that move at slightly different rates.

A difficult aspect of the resolution experiment is to distinguish between a system that measures rate of angle change and a system that resolves two motionless targets at different angles. One approach is to determine an angle-resolution cell such tha two small motionless targets cannot be resolved if they are both within the cell, and to perform all moving target experiments with objects that are not separated by more than a single angle resolution cell. For targets that move at a constant rate, the observation time must be limited to the time when the targets are close together.

3.3.4 Conclusion

In order to compensate for evasive maneuvers at close range, a sonar should be capable of determining the direction of cross-range movement when the sonar is close to the target. This capability exists in dolphin echolocation if two succeeding pulses can be coherently processed. A few more pulses may be necessary if suboptimal processing is used.

For some man-made sonar systems, a cross-range velocity estimate is relevant not only to measurement of evasive maneuvers but also to the use of target motion as a clutter rejection method.

Measurement of cross-range velocity is also important for tracking and beam-forming. The best boresight position for a future transmission can be predicted if a cross-range velocity estimate is available.

In the above applications, one would want to measure cross-range velocity at a long distance from the target. This measurement can be accomplished by increasing $SNR^{1/2}Tf_o d$ in (11), or by increasing $SNR^{1/2}TWd$ in (16).

To increase $SNR^{1/2}$, one can use pulse compression techniques with long signal durations. To increase d, one can gather data from two ends of a large towed array or (better still) from helicopter-dipped transducers that communicate with a central processor. For long target ranges, the signal duration T can be significantly increased. An increase in bandwidth W may be preferable to an increase in f_o, since attenuation increases with frequency.

The same bandwidth-array size trade-off that was found in Section 3.2 for target position measurement is again found in (16). Both angle and angle rate measurements can be improved by increasing array size or by increasing the bandwidth of the sonar system.

3.3.5 References for Section 3.3

1. K. D. Roeder, "Episodes in insect brains," Amer. Scientist 58, 378-389, 1970.

2. G. M. Anderson, "A model for the bat versus moth pursuit-evasion problem," paper to be presented at 96th meeting, Acous. Soc. Amer., Honolulu, Hawaii, November 27-December 1, 1978.

3. J. C. R. Licklider, Experientia 7, p. 128 (1951).

4. B. McA. Sayers and E. C. Cherry. "Mechanism of binaural fusion in the hearing of speech," J. Acous. Soc. Amer. 29, 1957, pp. 973-987.

5. R. A. Altes, "Sound localization, waveform estimation, and detection in a binaural system, with applications to multi-array processing," submitted to J. Acous. Soc. Am.

6. N. I. Durlach, "Equalization and cancellation theory of binaural masking-level differences," J. Acous. Soc. Am. 35, 1206-1218, 1963.

7. J. A. Simmons, "The resolution of target range by echo-locating bats," J. Acous. Soc. Amer. 54, 157-173.

8. R. A. Altes, "Signal reconstruction and detection from spectrograms, with applications to theories of hearing and animal echolocation," Section 2.2.

9. C. A. Stutt, "Some results on real-part/imaginary-part and magnitude-phase relations in ambiguity functions," IEEE Trans. Inform. Theory IT-10, 321-327, 1964.

10. C. E. Cook and M. Bernfeld, Radar Signals. New York: Academic, 1967.

11. D. R. Griffin, Listening in the Dark. New Haven: Yale, 1958.

12. R. A. Altes and E. L. Titlebaum, "Bat signals as optimally doppler tolerant waveforms," J. Acous. Soc. Amer. 48, 1014-1020.

13. R. A. Altes and W. D. Reese, "Doppler-tolerant classification of distributed targets–a bionic sonar," IEEE Trans. AES-11, 708-723, 1975.

14. R. A. Altes, "Sonar for generalized target description and its similarity to animal echolocation systems," J. Acous. Soc. Amer. 59, 97-105, 1976.

15. R. A. Altes and E. L. Titlebaum, "Graphical derivations of signals for radar, sonar, and communication," IEEE Trans. AES-11, 38-44, 1975.

16. R. A. Altes, "Optimum waveforms for sonar velocity discrimination," Proc. IEEE 59, 1615-1617, 1971.

17. R. A. Altes, "Methods of wideband signal design for radar and sonar systems," NTIS No. AD 732 494, 1971.

18. W. W. L. Au, R. W. Floyd, R. H. Penner, and A. E. Murchison, "Measurement of echolocation signals of the Atlantic bottlenose dolphin, Tursiops truncatus Montagu, in open waters," J. Acous. Soc. Am. 56, 1280-1290, 1974.

3.4 A Test of the Energy Spectrum Analysis (Johnson-Titlebaum) Hypothesis

3.4.1 Introduction to Section 3.4

R. A. Johnson and E. L. Titlebaum (1976) have proposed a model for echolocation processing that is related to the perception of time separation pitch. The proposed model forms the magnitude-squared Fourier transform of the transmitted pulse and an echo, i.e., transmitted and echo pulses are both included in the integration interval for Fourier analysis. For an echo with delay Δ and attenuation α, the resulting energy density spectrum is

$$|R(f)|^2 = |U(f)|^2 \left[1 + \alpha^2 + 2\alpha\cos(2\pi\Delta f)\right] \qquad (1)$$

where $U(f)$ is the Fourier transform of the transmitted signal. The presence of a target introduces a frequency domain ripple with period $1/\Delta$ Hz. Detection of a target and estimation of its range depend upon an analysis of this ripple.

In his thesis, R. A. Johnson (1972) has suggested that rippled noise could be very detrimental to the performance of an energy spectrum analyzer. In this section, we use locally optimum detection ideas to provide further insight into the effect of rippled noise.

3.4.2 Locally Optimum Detection Using the Energy Spectrum as Data

Our objective is to obtain a statistical test that can distinguish between the hypothesis H_1 that a target is present in additive Gaussian noise and the hypothesis H_0 that only Gaussian noise is present. Let $P_N(f)$ be the noise power spectral density. The expected form of the energy spectrum under the two hypotheses is then

$$H_0: \quad E\left\{|R(f) + N(f)|^2\right\} = |U(f)|^2 + P_N(f)$$

$$H_{1\Delta}: \quad E\left\{|R(f) + N(f)|^2\right\} = |U(f)|^2 [1+\alpha^2 + 2\alpha \cos(2\pi \Delta f)] + P_N(f). \tag{2}$$

where $H_{1\Delta}$ is the hypothesis that a target is present at range $c\Delta/2$, and N(f) is the Fourier transform of a sample function of the noise process.

One can obtain a set of uncorrelated samples of the energy spectrum by using samples that are $(4T)^{-1}$ Hz apart, where T is the integration time of the Fourier analyzer. Let z_j denote the sample at frequency f_j. The probability densities of z_j under the two hypotheses are then

$$p(z_j|H_0) = \sigma_j^{-2} \exp\left\{[-z_j - |U(f_j)|^2] / \sigma_j^2\right\} \cdot I_0[2\sqrt{z_j |U(f_j)|^2} / \sigma_j^2] \tag{3}$$

$$p(z_j|H_1) = \sigma_j^{-2} \exp\left\{\left\{-z_j - |U(f_j)|^2[1 + \alpha^2 + 2\alpha \cos(2\pi \Delta f_j)]\right\} / \sigma_j^2\right\} I_0\left\{2\sqrt{z_j |U(f_j)|^2[1 + \alpha^2 + 2\alpha \cos(2\pi\Delta f_j)]} / \sigma_j^2\right\}$$

where $\sigma_j^2 \equiv P_N(f_j)$.

We now define a signal-to-noise ratio parameter θ, where

$$\theta = \alpha/\sigma_j. \tag{4}$$

Replacing $I_0(\cdot)$ by its power series representation, we have

$$p(z_j|H_0) = \sigma_j^{-2} \exp\left\{[-z_j - |U(f_j)|^2]/\sigma_j^2\right\} [1 + |U(f_j)|^2 z_j/\sigma_j^4 + \ldots]$$

$$p(z_j|H_{1\Delta}) = \sigma_j^{-2} \exp\left\{-\sigma_j^{-2} z_j - |U(f_j)|^2[\sigma_j^{-2} + \theta^2 + 2\sigma_j^{-1}\theta\cos(2\pi\Delta f_j)]\right\}$$
$$\cdot\left\{1 + \sigma_j^{-2} z_j |U(f_j)|^2[\sigma_j^{-2}+\theta^2 + 2\sigma_j^{-1}\theta\cos(2\pi\Delta f_j)] + \ldots\right\} .$$

The log likelihood ratio for M independent samples is

$$\ln \Lambda = \ln[\prod_{j=1}^{M} p(z_j|H_{1\Delta})/\prod_{j=1}^{M} p(z_j|H_0)].$$

The locally optimum test for deciding between $H_{1\Delta}$ and H_0 (Capon, 1961; Middleton, 1966) is to compare

$$(d/d\theta)\ln \Lambda_\theta\Big|_{\theta=0}$$

with a threshold, where

$$(d/d\theta)\ln \Lambda_\theta\Big|_{\theta=0} = \sum_{j=1}^{M}[-2\sigma_j^{-1}|U(f_j)|^2\cos(2\pi\Delta f_j)]$$
$$+ \sum_{j=1}^{M}\frac{[2\sigma_j^{-3} z_j |U(f_j)|^2\cos(2\pi\Delta f_j)]}{1+\sigma_j^{-4} z_j |U(f_j)|^2} . \quad (5)$$

The part of (5) that is independent of the data z_j can be incorporated into a threshold level. The locally optimum test is then to compare

$$l(\underline{z}) = \sum_{j=1}^{M} a_j z_j \cos(2\pi\Delta f_j) \quad (6)$$

with a threshold, where

$$a_j = 2\sigma_j^{-3}|U(f_j)|^2/[1+\sigma_j^{-4} z_j |U(f_j)|^2]$$

and

$$\sigma_j^2 = P_N(f_j).$$

The total number M of frequency domain samples increases with signal bandwidth. The likelihood ratio thus involves two non-central chi-square distributions with degrees of freedom that depend upon signal bandwidth. The locally optimum detector in (6) (and the maximum likelihood estimator for the delay parameter Δ) will involve correlation of the sampled energy spectrum with a vector that exhibits a hypothetical ripple, i.e., Fourier analysis of the energy spectrum.

If $P_N(f)$ in (2) has a ripple similar to that in (1), then similar energy density spectra will be observed under both hypotheses and it will be difficult to distinguish between then.

3.4.3 Effect of Rippled Noise Upon a Matched Filter

A matched filter has an expected output noise power P_{MF}, where

$$P_{MF} = \int_{-\infty}^{\infty} P_N(f) \, |U(f)|^2 \, df \tag{7}$$

under both hypotheses. A ripple in $P_N(f)$ will not greatly affect P_{MF} if $|U(f)|^2$ is smooth and broadband (as is the case for many dolphin clicks and FM bat pulses). Specifically, a periodic ripple in $P_N(f)$ with period $1/\Delta$ Hz will have very small effect upon the integral in (7) if

$$1/\Delta << B_u \tag{8}$$

where B_u is the signal bandwidth. An adaptable whiten-and-match filter will, in fact, take advantage of the nulls in a rippled noise power spectral density $P_N(f)$ in order to improve detection performance.

3.4.4 Experimental Procedure for Testing the Johnson-Titlebaum Model Against the Matched Filter Model

Assuming that the Johnson-Titlebaum model is implemented by an echolocating animal, broadband masking noise will be especially effective if the noise has power spectral density

$$P_N(f) = (N_o/2)\ [1 + \alpha^2 + 2\alpha\cos(2\pi\Delta f)] \qquad (9)$$

where Δ is the delay that is associated with the target. Masking noise with the power spectral density in (9) should have a much greater effect upon the energy spectral density model than white noise with the same average power. The appropriate noise process can be generated by passing white noise through an attenuator and a delay line, and by adding the attenuated, delayed noise to the original noise process.

The noise can be transmitted toward the animal from behind a small target which the animal attempts to detect. Detection performance should be maximally degraded when Δ in (9) is equal to the delay between transmitted pulse and echo, and there should be less degradation for other values of Δ.

If the matched filter model is correct, then performance degradation should be independent of the parameter Δ in (9), provided that condition (8) holds.

The same masking noise can be used for human subjects who are attempting to estimate time separation pitch or to discriminate a single pulse from a pulse pair, where the second pulse has smaller amplitude than the first. These tests can be used to verify our prediction that a rippled noise spectrum is especially disturbing to a detection and range estimation process that uses energy spectral analysis.

A reasonable experimental procedure has two steps:

1. Given two broadband pulses $u(t) + \alpha u(t - \Delta_1)$, find the threshold value of α in human subjects such that the second pulse is detected (say) 75% of the time in a white noise background. Call this value α_w. Also find the threshold value of α for detection of the second pulse in a rippled noise background with $P_N(f)$ as in (9), such that $P_N(f)$ has the same average power as the white noise. Call this value α_r. Evaluate the effect of rippled noise upon human estimation of time separation pitch when $\alpha = 1$.

   If $\alpha_r > \alpha_w$ and/or if the rippled noise in (9) maximally degrades the estimation of time separation pitch when $\Delta = \Delta_1$, proceed to the following experiment.

2. Evaluate the effect of masking noise with rippled power spectral density as in (9) upon target detection and range estimation performance of dolphins and bats. Use white noise with the same average power and a sequence of different Δ-values in (9) for comparison.

3.4.5 Conclusion

Both intuition and a locally optimum detector formulation indicate that, to detect a target from an energy spectrum that includes the transmitted signal as well as hypothetical echoes, one should perform a Fourier analysis of the energy spectrum. Such an analysis is susceptible to rippled noise, i.e., a noise power spectrum that is modulated with a periodic function. If the period of this ripple is small relative to signal bandwidth, then the ripple

will not greatly affect the performance of a matched filter. This analysis leads to a straightforward behavioral test that can be used to decide whether matched filtering or energy spectrum analysis is a better model for animal echolocation.

3.4.6 References for Section 3.4

1. Capon, J. (1961). "On the asymptotic efficiency of locally optimum detectors," IRE Trans. on Inform. Theory, vol. IT-7, 67-71.

2. Johnson, R. A. (1972). "Energy spectral analysis as a processing mechanism for echolocation," Ph.D. dissertation, Univ. of Rochester.

3. Johnson, R. A., and Titlebaum, E. L. (1976). "Energy spectrum analysis: A model of echolocation processing," J. Acous. Soc. Am. 60, 484-491.

4. Middleton, D. (1966). "Canonically optimum threshold detection," IEEE Trans. on Inform. Theory, vol. IT-12, 230-243.

3.5 Summary and Conclusion for Volume 3

The use of extremely wide bandwidths by dolphins and some bats is helpful for target classification and interference suppression, if the techniques in Volumes 1 and 2 are employed. In this volume, we have shown that wide signal bandwidths can also be used to compensate for limited array size. The trade-off between bandwidth and array size applies both to target localization and to the measurement of tangential (cross-range) velocity.

The locally optimum detection approach, which leads to a spectrum correlator, can also be applied to an energy spectrum representation of echo data. This application suggests that R. A. Johnson's energy spectrum analyzer model for animal echolocation should be especially susceptible to a rippled noise background. *Johnson's thesis* contains a similar suggestion. It follows that one can test the energy spectrum analysis model against a stored-replica matched filter model by comparing echolocation performance in white noise and in rippled noise.